Aspects of Entanglement in Multipartite and Decaying Systems

DISSERTATION

zur Erlangung des Grades

eines Doktors der Naturwissenschaften

vorgelegt von

M.Sc. Marius Paraschiv

geb. am 12.08.1989 in Bukarest

eingereicht bei der Naturwissenschaftlich-Technischen Fakultät

der Universität Siegen

Siegen 2016

Gutachter:

- Prof. Dr. Otfried Gühne

- Prof. Dr. Thomas Mannel

Datum der mündlichen Prüfung: 25.11.2016

Prüfer:

- Prof. Dr. Otfried Gühne (Vorsitz der Prüfungskommision)

- Prof. Dr. Thomas Mannel

- Prof. Dr. Mario Agio

- Prof. Dr. Christof Wunderlich

Abstract

The study and characterisation of quantum entanglement represents an extended effort within the field of quantum information. This thesis addresses two problems. The first regards entanglement in open systems, where it's more difficult to define a dichotomic (two outcome) observable due to population loss. The second problem concerns genuine multipartite entanglement, that is entanglement between many particles in states that cannot be separable with respect to any possible bipartition of a system.

The first chapter consists of an introduction to the basic elements of quantum mechanics and quantum information theory. We briefly describe a few historical facts about quantum mechanics and the study of entanglement, to help put things into perspective.

The second chapter is a detailed discussion of the neutral kaon system. These particles are produced in pairs and are described as a particle-antiparticle system. This system displays some unique properties like the violation of CP-symmetry, and shares some characteristics with other mesons, such as neutral particle oscillation and decay. This makes formulating Bell-type inequalities for them more difficult, but also provides the opportunity for new tests.

The third chapter continues with the presentation of an already existent effective formalism for performing Bell tests on neutral kaons. The essence of the formalism is a switch to the Heisenberg picture, transferring the time evolution and dependence on measurement directions to a so-called effective operator. This has many advantages, some of the most important being a proper normalization during population loss (due to decay), an easy application to the case of multiple particles and the fact that it allows one to observe entanglement within the system for a relatively long amount of time. The final part presents a way to simulate neutral kaons with atomic systems, namely with Ytterbium isotopes and discuss what are the differences between these atomic systems and neutral kaons.

The second part of the thesis treats the problem of proving genuine multipartite entanglement from separable two-body marginals. For this, an introduction to semidefinite programming is necessary due to the fact that the problem under study can be formulated in terms of this method. We will briefly discuss linear and semidefinite programming as well as the concept of duality and provide some basic examples.

The formal description of this problem and previous results are provided in the fifth

chapter. Our result shows that, through a cyclic iteration between two SDPs, one obtains states with the desired properties. Using this method we managed to go up to six qubit states for various configurations. From this we can construct higher-dimensional states having the same properties.

Zusammenfassung

Die Studium und die Charakterisierung von Verschränkung in Quantensystemen ist ein beständiges Ziel in dem Gebiet der Quantuminformationstheorie. Diese Dissertation widmet sich hauptsächlich zwei Problemen: Einerseits dem Studium von Verschränkung in offenen Quantensystemen, wo die Definition einer dichotomischen Observablen wegen Teilchenverlust im System gewisse Schwierigkeiten bereitet. Andrerseits untersucht es echte Mehrteilchen-Verschränkung, welches Verschränkung in Zuständen beschreibt, welche bezüglich aller möglichen Bipartitionen nicht separabel sind.

Das erste Kapitel führt in die grundlegenden Elemente der Quantenmechanik und der Quanteninformationstheorie ein. Um den Kontext darzustellen beschreiben wir kurz die historische Entwicklung der Quantenmechanik und im Spezifischen die des Phänomens Verschränkung.

Das zweite Kapitel beinhaltet eine detaillierte Diskussion von neutralen Kaon-Systemen. Die Teilchen entstehen in Prozessen als Paare, und lassen sich als Teilchen-Antiteilchen beschreiben. Zudem zeigen diese Systeme einige Besonderheiten, im speziellen die Verletzung der CP-Symmetrie, und teilt im weiteren einige Merkmale mit anderen Mesonen, wie zum Beispiel die neutrale Teilchen-Oszillation und Teilchenzerfall. All dies macht die Formulierung von Bell-artigen Ungleichen anspruchsvoller, andrerseits bietet sich dadurch die Möglichkeit von neuen Experimenten.

Das dritte Kapitel präsentiert den bereits existierenden effektiven Formalismus, um Bell-Experimente mit neutralen Kaonen durchzuführen. Einer der Hauptaugenmerke des Formalismus ist der Wechsel ins Heisenberg-Bild, welches die Zeitentwicklung und die Abhängigkeiten zu den Messrichtungungen in den sogenannten effektiven Operator verschiebt. Dies hat viele Vorteile, wobei als einer der wichtigsten die korrekte Normierung bezüglich Teilchenverlust ist. Weiterhin vereinfacht dies die Anwendung auf Mehrteilchen-Verschränkung und gibt die Möglichkeit einer verlängerten Beobachtungsdauer. Zuletzt wird diskutiert, wie sich neutrale Kaonen durch atomare Systeme, namentlich durch Ytterbium Isotope, simulieren lassen, bevor Unterschiede zwischen diesen atomaren Systemen und neutralen Kaonen erörtert werden.

Der zweite Teil der Dissertation untersucht das Problem, echte Mehrteilchen-Verschränkung

nur durch separable zwei-Teilchen Marginalien zu zeigen. Wir führen dazu in die Methode der semidefinite Programmierung (SDP) ein, und diskutierern sowohl lineare und semidefinite Programmierung als auch das Konzept der Dualität. Weiterhin geben wir einige einfach Beispiele.

Eine detaillierte Darstellung dieses Problems sowie bereits bekannte Herangehensweisen erscheinen im fünften Kapitel. Unser Resultat zeigt, dass eine zyklische Iteration zwischen zwei semidefiniten Programmen einen Zustand findet, welcher echt mehrteilchen-verschränkt ist, jedoch separable zwei-Teilchen Marginalien hat. Durch diese Methode finden wir Zustände mit von bis zu sechs qubits, welche diese Eigenschaften haben. Aus diesen können dann wiederum höherdimensionale Zustände gebildet werden, welche auch separable zwei-Teilchen Marginalien aufweisen, jedoch echt mehrteilchen-verschränkt sind.

Contents

I.   Introduction

Since its beginnings, at the start of the 20th century, quantum mechanics has expanded to encompass a large array of domains within physics. Almost every field of modern physics has quantum laws at its foundations or is an extension of an already existent classical field to the quantum realm.

By the third decade after its birth (commonly associated with Max Planck's publication of his black-body radiation law, in 1901), quantum mechanics had already managed to explain much of the existing phenomenology. It went on to explain atomic and nuclear structures and ultimately become the foundation of the standard model of particles and interactions. It also found more pragmatic applications, like in the study of semiconductors, bringing with them a revolution in automation and information technology.

In spite of its huge successes, however, quantum mechanics has also left open fundamental questions, with which physicists have struggled for the last hundred years. What exactly does the word "measurement" mean within a quantum mechanical context? Why is the macroscopic world behaving in a classical way? (following the rules of classical not quantum physics) Is the quantum state real or just a mathematical object? A number of unanswered questions were not the only problems physicists had to deal with. quantum mechanics seemed to display a series of strange behaviours like wave-particle duality and, non-locality.

The Principle of Locality states that two spatially-separate systems can interact with each other only through a mediator (field or particle), and that the interaction has a finite speed. Thus there cannot be any instantaneous action at a distance. In a seminal paper in 1935, Einstein, Podolsky and Rosen [19], together with later work by Bell [2], have shown that Quantum Mechanics might not be a local theory, as we shall see in the next section.

A.   The EPR Argument

Due to its non-classical predictions, various aspects of the theory were under scrutiny from the very beginning. In their 1935 paper, Einstein, Podolsky and Rosen [19] sought to prove that the physical description of a system, given by the quantum wave-function cannot be complete. Before describing their argument in detail, we must first give two definitions.

Definition I.1. *A theory is considered complete if every element of physical reality has a counterpart in the theory.*

Definition I.2. *If the value of some physical quantity can be predicted with certainty, without disturbing the system, then to that quantity there corresponds an element of physical reality.*

First, one can consider the case of a single particle. Take two incompatible observables, say position $\vec{x}$ and momentum $\vec{p}$. One can measure either $\vec{x}$ or $\vec{p}$, but not both at the same time. This brings forth two possibilities:

- if both $\vec{x}$ and $\vec{p}$ are real, then the wave function ψ is not a complete description of the system's state. Say the observer measures the position of the particle. Then he does not now precisely the value for the momentum, even though the momentum itself is an element of physical reality.

- only the measured observable, say $\vec{x}$ is real, and the other is created at the moment of measurement. This could lead one to conclude that ψ is complete.

In order to go one step further, the discussion is simplified if, instead of the continuous observables position and momentum, we choose two spin directions, corresponding to σ_z and σ_x. Then we can easily write down the state for the two parties (from now on, keeping with convention, the two experimenters will be referred to as Alice and Bob).

$$|\psi_{AB}\rangle = \frac{1}{\sqrt{2}}(|0_A, 1_B\rangle + |0_B, 1_A\rangle). \tag{1}$$

Suppose Alice measures the spin along σ_z on her qubit. She them immediately knows that Bob's qubit is in either a $|0\rangle$ or a $|1\rangle$ state, depending on her measurement outcome. If, however, Alice chooses to measure σ_x ,then she knows Bob's qubit is in one of the two σ_x eigenvectors,

$$|0_x^B\rangle = \frac{1}{\sqrt{2}}(|0^B\rangle + |1^B\rangle),$$
$$|1_x^B\rangle = \frac{1}{\sqrt{2}}(|0^B\rangle - |1^B\rangle). \tag{2}$$

By her choice of either the σ_z or σ_x observable, Alice can predict one of two incompatible properties of Bob's qubit. Due to the fact that the two Pauli operators do not commute,
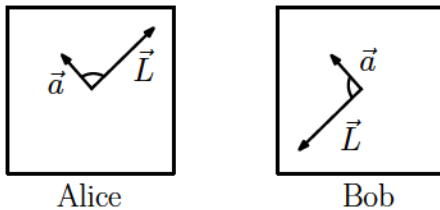
FIG. 1: Anticorrelations in arbitrary directions without quantum mechanics.

hence they have no common eigenstates, there is no quantum state having well-defined values for both σ_z and σ_x. Thus, there need to be at least two distinct wave functions describing what seems to be the same situation [1], hence the wave function is an incomplete description of physical reality.

Assumption 1. *In the above argument it was assumed that the principle of locality holds, meaning that measurements on one particle do not instantaneously lead to a change in the state of the second particle.*

As we shall see, keeping this line of reasoning will lead to a contradiction.

Note that, contrary to the common misconception that anticorrelations in arbitrary directions are a profoundly quantum mechanical phenomenon, they can be entirely reproduced within classical physics. Consider the case of two spinning tops in two boxes (Fig.1), prepared such that their angular momenta have opposite directions. By defining a "spin" operator for any arbitrary direction $\vec{a}$,

$$S(\vec{a}) = \text{sign}(\vec{a} \cdot \vec{L}), \tag{3}$$

we obtain perfect anticorrelations in arbitrary directions without quantum mechanics.

A first answer to EPR was given the same year by Bohr [7]. Bohr's main focus was first on criticizing the EPR definition of "reality" and second on arguing that, while measuring only one observable, say $\vec{x}$ or $\vec{p}$ on one particle, only the corresponding observable of the other particle can be real. The issue is that Bohr does not also discuss any influence between the particles, which seems to be implied, if Bob's particle "knows" which measurement was performed by Alice.

---

[1] Both σ_z and σ_x are elements of physical reality, since Alice can predict the state of Bob's qubit without disturbing his system, in accordance with Definition I.2.
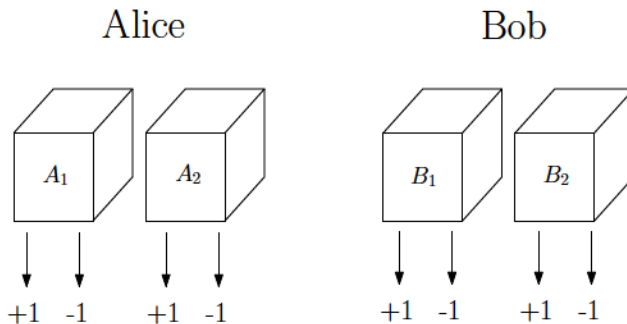
FIG. 2: Two-party basic setup for Bell inequalities. Alice and Bob can perform measurements on two observables each and the results of any measurement can be ±1.

B.   Local Hidden Variables and Bell Inequalities

We will try now to make quantum mechanics complete, in the EPR sense by adding extra parameters that, though not accessible to the experimenter, help the wave function describe the full properties of the system. Such a theory is called a "hidden-variable theory", and the inaccessible parameters are called "hidden variables". Furthermore, because it seems reasonable to expect that the complete version of quantum mechanics must also be compatible with the theory of special relativity, the principle of locality must also hold. Therefore we address here a class of theories known as "local hidden-variable theories", and we shall see that these theories are not compatible with experimental predictions. In this, and the following sections on entanglement and entanglement witnesses, we shall mainly follow Ref.[24].

Consider the situation depicted in Fig.2. Alice and Bob perform simultaneous measurements on four quantities,A_1 and A_2 for Alice and B_1 and B_2 for Bob, M times. The measurement outcomes will be labelled by a_1, a_2, b_1 and b_2, respectively. The expectation values can simply be obtained by averaging the results

$$\langle A_i, B_j \rangle = \frac{1}{M} \sum_{k=1}^{M} a_i(k) b_j(k). \tag{4}$$

If the probabilities for the outcomes can be written as

$$p(a_1^+, b_2^-) = p(a_1 = +1, b_2 = -1), \tag{5}$$

then one can write the expectation values as

$$\langle A_i B_j \rangle = p(a_i^+, b_j^+) - p(a_i^-, b_j^+) - p(a_i^+, b_j^-) + p(a_i^-, b_j^-). \tag{6}$$

4

One can now introduce the idea of a Local Hidden-Variable model (LHV). Two assumptions need to be made: first, the measurement results should be independent of whether they are actually measured or not (this corresponds to the reality assumption), second, Alice's results should not depend on Bob's choice of observables and vice-versa (locality assumption).

With the above in mind, one can make an ansatz for the probabilities

$$p(a_i^\alpha, b_j^\beta) = \int d\lambda p(\lambda) A_\lambda(a_i^\alpha) B_\lambda(b_j^\beta), \tag{7}$$

where α and β denote the possible outcomes ± 1 and λ is the hidden variable, occurring with probability $p(\lambda)$. The response function $A_\lambda(a_i^\alpha) B_\lambda(b_j^\beta)$ factorizes due to the locality assumption. One can always assume an LHV model to be deterministic (i.e. for a given lambda, $A_\lambda(a_i^\alpha)$ and $B_\lambda(b_j^\beta)$ take only the values of 0 or 1). A nondeterministic model corresponds to a deterministic one where λ is not known [42, 54].

In 1964, Bell [2] showed that there are bounds on the correlations of these probabilities. We present here a slightly more general bound, obtained by Clauser and Horne [13],

$$p(a_1^-, b_1^-) + p(a_1^+, b_2^-) + p(a_2^-, b_1^+) - p(a_2^-, b_2^-) \geq 0. \tag{8}$$

From this, one can derive the Clauser-Horne-Shimony-Holt (CHSH) inequality [14, 15],

$$\langle A_1 B_1 \rangle + \langle A_2 B_1 \rangle + \langle A_1 B_2 \rangle - \langle A_2 B_2 \rangle \leq 2. \tag{9}$$

It is important to notice that, while deriving Eq. (9), there were no notions of quantum mechanics involved, so we must now place the CHSH inequality in a quantum context.

Consider the two experimenters, Alice and Bob, each having a spin-$\frac{1}{2}$ particle, on which they can perform the measurements A_i and B_j, corresponding to measuring the Pauli spin operators σ_x and σ_y, respectively. One may now write the inequality in operator (or witness) form by defining a Bell operator

$$\mathcal{B} = A_1 \otimes B_1 + A_2 \otimes B_1 + A_1 \otimes B_2 - A_2 \otimes B_2. \tag{10}$$

There are quantum states that violate this inequality and give a value of $2\sqrt{2}$, the so-called Tsirelson bound [12], which can also be shown to be the maximal violation for the CHSH.

For a choice of observables

$$A_1 = -\sigma_x$$
$$A_2 = -\sigma_y$$
$$B_1 = \frac{(\sigma_x + \sigma_y)}{2} \qquad (11)$$
$$B_2 = \frac{(\sigma_x - \sigma_y)}{2}$$

the state with the highest violation of the CHSH inequality is the eigenstate of the Bell operator $\mathcal{B}$, corresponding to the largest eigenvalue,

$$|\psi\rangle = \frac{1}{\sqrt{2}}(|01\rangle - |10\rangle), \qquad (12)$$

also known as the singlet state.

We have seen that quantum mechanics violates Bell inequalities and this is due to the fact that one of the two assumptions initially made, reality or locality, is wrong. It is not at all obvious which one. Removing the realism conditions and making certain assumptions on the correlation functions $\langle A_i, B_j \rangle$, it is possible to derive Bell-type inequalities [31]. Conversely, one can keep realism and remove the locality assumption, obtaining a non-local theory compatible with quantum mechanics, such as Bohmian mechanics. For a more detailed discussion see Ref. [24].

C.   A Different Kind of Bell Inequality

One Bell-type inequality we will be focusing on in later chapters was initially proposed by C. Sliwa [46] and shown by D. Collins and N. Gisin [17] not to be equivalent with the CHSH. For brevity we shall call this the Sliwa-Collins-Gisin inequality or SCG.

This is a two-party three-setting inequality of the form

$$\langle A_1 \rangle + \langle A_2 \rangle + \langle B_1 \rangle + \langle B_2 \rangle + \langle A_1 B_1 \rangle + \langle A_1 B_2 \rangle + \langle A_2 B_1 \rangle$$
$$+\langle A_2 B_2 \rangle + \langle A_3 B_1 \rangle - \langle A_3 B_2 \rangle + \langle A_1 B_3 \rangle - \langle A_2 B_3 \rangle \geq -4. \qquad (13)$$

Here the $\langle A_i \rangle$ and $\langle B_j \rangle$ should be understood as $\langle A_i \otimes \mathbb{1} \rangle$ and $\langle \mathbb{1} \otimes B_j \rangle$, respectively. This means that the correlation functions belong to the case where only one of the observers performs a measurement.

In Ref. [17], an example state has been given

$$\rho = 0.85 P_{|\psi\rangle} + 0.15 P_{|01\rangle}, \tag{14}$$

where $P_{|\psi\rangle}$ is the projector corresponding to the state

$$|\psi\rangle = \frac{1}{\sqrt{5}}(2\,|00\rangle + |11\rangle), \tag{15}$$

and $P_{|01\rangle} = |01\rangle\,\langle 01|$. This state does violate the SCG inequality but not the CHSH, proving that there is a class of states which are only detected by the SCG, thus the two Bell-type inequalities are not equivalent.

D. Violation of Bell-type Inequalities and Entanglement

Violation of Bell-type inequalities directly implies entanglement. Before explaining this, it would be appropriate here to give a formal definition of entanglement.

Definition I.3. *Let ρ be the density matrix of a bipartite system. ρ is a product state if $\rho = \rho_A \otimes \rho_B$, where ρ_A and ρ_B are the reduced density matrices for Alice and Bob, respectively. Furthermore, if the global state can be written as $\rho = \sum_i p_i \rho_A^i \otimes \rho_B^i$, the state is called separable, where $\sum_i p_i = 1$ and $p_i \geq 0$ for all i.*

Definition I.4. *A state that is not separable is called entangled.*

We stated above that any separable state can be written in the form

$$\rho = \sum_i p_i \rho_A^i \otimes \rho_B^i. \tag{16}$$

The correlation function for bipartite measurements A_i and B_j will thus be given by

$$\langle A_i B_j \rangle = \sum_k p_k Tr(A_i \rho_A^k) Tr(B_j \rho_B^k). \tag{17}$$

Defining two operators

$$\begin{aligned} \mathcal{U}_k(A_i) &= Tr(A_i \rho_A^k), \\ \mathcal{B}_k(B_j) &= Tr(B_j \rho_B^k), \end{aligned} \tag{18}$$

leads to the following form of the correlation function

$$\langle A_i B_j \rangle = \sum_k p_k \mathcal{U}_k(A_i) \mathcal{B}_k(B_j), \tag{19}$$

which is exactly the case of LHV models (See Eq.(7)). This means that, if a quantum state violates a Bell-type inequality, it cannot be a separable state, hence it's entangled. The opposite is generally not true, Bell inequalities are not optimal entanglement witnesses, so there exist entangled states that they do not detect [24].

E. Partial Transposition and a Criterion for Entanglement Detection

In the following, we will briefly present an entanglement detection criterion, known as the positive partial transpose (PPT) criterion. It is worth mentioning that there is a large number of entanglement criteria available in the literature but we restrain our discussion only to what will be applicable in later chapters.

Any density matrix of a composite system can be expanded as

$$\rho = \sum_{i,j}^{N} \sum_{k,l}^{M} \rho_{ij,kl} \, |i\rangle \langle j| \otimes |k\rangle \langle l| , \tag{20}$$

in terms of some chosen product basis.

Definition I.5. *The partial transposition of ρ is defined as the transposition with respect to one of the subsystems. Its effect, on Alice's system, is described by $\rho^{T_A} = \sum_{i,j}^{N} \sum_{k,l}^{M} \rho_{ji,kl} \, |i\rangle \langle j| \otimes |k\rangle \langle l|$ and on Bob's system, $\rho^{T_B} = \sum_{i,j}^{N} \sum_{k,l}^{M} \rho_{ij,lk} \, |i\rangle \langle j| \otimes |k\rangle \langle l|$.*

A useful property of the partial transpose is that $\rho^T = (\rho^{T_A})^{T_B}$, or $\rho^{T_B} = (\rho^{T_A})^T$.

Definition I.6. *A density matrix ρ has positive partial transpose (or simply, is PPT) if $\rho^{T_A} \geq 0$ or, equivalently, $\rho^{T_B} \geq 0$.*

Now we are ready to state the Peres-Horodecki criterion (also known as the PPT criterion) [41].

Theorem I.1. *If ρ is a bipartite separable state, then ρ is PPT.*

Proof. If ρ is separable, it can be written as $\rho = \sum_k p_k \rho_A^k \otimes \rho_B^k$. Taking the partial transpose of this, with respect to Alice's system, gives $\rho^{T_A} = \sum_k p_k (\rho_A^k)^T \otimes (\rho_B^k) = \sum_k p_k \tilde{\rho}_A^k \otimes \rho_B^k$. □

8

In general, the converse of this is not true in higher dimensions. In later chapters we will be dealing with 2×2 systems and, in this special case, the following theorem, known as the Horodecki theorem [25] holds.

Theorem I.2. *If ρ is a state of a 2×2 or 2×3 system, $\rho^{T_A} \geq 0$ implies separability.*

F.   Entanglement Witnesses and Multipartite Entanglement

While it is not the purpose of this section to give an in-depth review of entanglement witnesses and their construction (for that see, for example Ref. [24][26]), we will give here the formal definition of an entanglement witness and, at the end of the section, discuss an important class of witnesses called fully-separable witnesses, that will prove important later on.

Definition I.7. *An observable W is called an entanglement witness (or just witness) if*

$$
\begin{aligned}
Tr(W\rho_S) \geq 0 \qquad &\forall \rho_S \text{ separable}, \\
Tr(W\rho_e) < 0 \qquad &\text{for at least one entangled } \rho_e.
\end{aligned}
\tag{21}
$$

An important remark, stated here without proof (for proof see Ref. [25]) is that for any entangled state ρ_e there exists a witness that detects it.

As an example [24] of a two-qubit entanglement witness, one can easily be constructed by using the PPT criterion. Consider a state ρ_e which is NPT (negative partial transpose), hence it does have a negative eigenvalue $\lambda_- < 0$ to which there corresponds an eigenvector $|\eta\rangle$. The witness $W = |\eta\rangle \langle \eta|^{T_A}$ detects ρ_e since $\text{Tr}(W\rho_e) = \text{Tr}(|\eta\rangle \langle \eta|^{T_A} \rho_e) = \text{Tr}(|\eta\rangle \langle \eta| \rho_e^{T_A}) = \lambda_- < 0$.

In order to generalize entanglement to the multipartite case, we must first look at two types of pure states for a three-qubit system. The first type is given by fully separable states, which can be written as

$$
|\psi^{fs}\rangle = |\alpha_A\rangle \otimes |\beta_B\rangle \otimes |\gamma_C\rangle,
\tag{22}
$$

while the second represents biseparable states,

$$
|\psi^{bs}\rangle = |\alpha_A\rangle \otimes |\delta_{BC}\rangle,
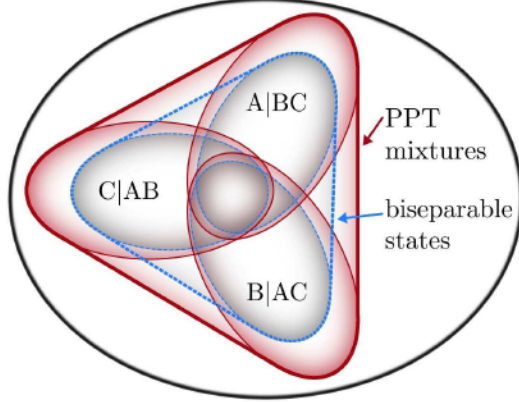\tag{23}
$$

FIG. 3: Graphical representation of the sets of biseparable states and PPT mixtures. (Picture reproduced from [29])

with respect to bipartition $A|BC$ of the system.

In the case of mixed states, a state ρ_{ABC} is said to be *separable with respect to a bipartition* $A|BC$ if it can be written as a mixture of product states, with respect to the bipartition $A|BC$

$$\rho_{A|BC}^{sep} = \sum_k q_k \left| \phi_A^k \right\rangle \left\langle \phi_A^k \right| \otimes \left| \psi_{BC}^k \right\rangle \left\langle \psi_{BC}^k \right|. \tag{24}$$

If the global state of the system can be written as

$$\rho^{bs} = p_1 \rho_{A|BC}^{sep} + p_2 \rho_{B|AC}^{sep} + p_3 \rho_{C|AB}^{sep} \tag{25}$$

it is known as *biseparable*. Now we can proceed with defining genuine multipartite entanglement.

Definition I.8. *If a state is not biseparable, thus it cannot be written in the form of Eq.(25), then it is genuinely multipartite entangled.*

One last class of states we need to look at is represented by the so-called PPT-mixtures. Similarly to biseparable states, a state that can be written as

$$\rho^{pmix} = p_1 \rho_{A|BC}^{ppt} + p_2 \rho_{B|AC}^{ppt} + p_3 \rho_{C|AB}^{ppt} \tag{26}$$

in terms of states PPT with every bipartition of the system, are known as *PPT mixtures*. The reason for discussing PPT-mixtures here is that (see Fig.3) PPT-mixtures include biseparable

states, thus, if a state is not a PPT-mixture, it certainly is genuinely multipartite entangled. It is much easier to prove that a state is not a PPT-mixture, due to the ease of implementation of the PPT criterion, than to prove that the state is not biseparable.

In the last part of this section, a class of entanglement witnesses is presented, that proves useful in the case of PPT-mixtures. For a two-particle case, A and B, a witness W is called *decomposable* if it can be written in terms of two positive semidefinite observables P and Q ($P \geq 0$ and $Q \geq 0$) as

$$W = P + Q^{T_A}, \tag{27}$$

where T_A represents the partial transpose with respect to subsystem A. If one generalizes this definition to a multipartite case, namely, a witness that can be written as

$$W = P_M + Q_M^{T_M}, \tag{28}$$

for any bipartition $M|\bar{M}$, of the system, then the witness W is called *fully decomposable*.

Theorem I.3. *If ρ is not a PPT mixture, then there exists a fully decomposable witness W that detects it. The proof can be found in Ref. [29].*

G.   Applications of Entanglement

In this section we will describe two such applications, one is quantum cryptography, more exactly the problem of securely distributing a private key (a problem also known as quantum key distribution) between two parties, and a second application is the quantum teleportation scheme, used to transmit a qubit state between the same two parties.

1.   Quantum Key Distribution

One of the first key distribution protocols in quantum information was the BB84 protocol [3]. It consists of two observers, Alice and Bob, sharing a private key over a public channel, as part of a private key system. The protocol also allows the two to verify if their communication has been intercepted by an eavesdropper, aptly named Eve, thus compromising their security. One requirement for the implementation of the BB84 protocol is that Alice and Bob can exchange qubits over a public channel, with an error rate that is sufficiently small.

String Values	$b_k = 0$	$b_k = 1$
$a_k = 0$	$\lvert\uparrow\rangle$	$\lvert\nearrow\rangle$
$a_k = 1$	$\lvert\rightarrow\rangle$	$\lvert\searrow\rangle$

TABLE I: Alice's encryption rule in the BB84 protocol.

To describe the scheme, we primarily follow the derivations from Ref. [1, 37]. Alice beginns with two strings of random classical bits a and b, of equal length. She encodes each bit in a as $\{\lvert0\rangle, \lvert1\rangle\}$, if the corresponding bit in string b is 0 and $\{\lvert+\rangle, \lvert-\rangle\}$, if the corresponding bit in string b is 1, where

$$
\begin{aligned}
\lvert+\rangle &= \frac{1}{\sqrt{2}}(\lvert0\rangle + \lvert1\rangle), \\
\lvert-\rangle &= \frac{1}{\sqrt{2}}(\lvert0\rangle - \lvert1\rangle),
\end{aligned}
\tag{29}
$$

are the eigenvectors of the Pauli σ_X matrix.

After the encoding operation, Alice is left with the state

$$
\lvert\psi\rangle = \bigotimes_k \lvert\psi_{a_k b_k}\rangle,
\tag{30}
$$

with a_k being the k-th bit of string a, which can be in one of the four possible states $\{\lvert0\rangle, \lvert1\rangle, \lvert+\rangle, \lvert-\rangle\}$. Consider now two photon polarization bases $\{\lvert\uparrow\rangle, \lvert\downarrow\rangle\}$, representing vertical and horizontal polarization and $\{\lvert\nearrow\rangle, \lvert\searrow\rangle\}$, representing a polarization basis rotated by 45 degrees with respect to the first one. We denote the two bases as $Z = \{\lvert\uparrow\rangle, \lvert\downarrow\rangle\}$ and $X = \{\lvert\nearrow\rangle, \lvert\searrow\rangle\}$, and we identify the four basis vectors with the eigenkets of the Pauli σ_z and σ_x, respectively.

Thus, the value of the k-th bit in string b, say b_k, gives the choice of basis (Z or X) for encoding the k-th bit in string a, a_k. In it's turn, the value of the corresponding a_k bit gives the ket that Alice will use during the encoding process. To make this clearer, the rule for Alice's choice of kets is described in Table I.

After obtaining her encrypted state, Alice sends it to Bob. Since, at this point, Bob has no knowledge of string b, all the can do is measure all the qubits received from Alice, and changing the measurement basis between Z and X randomly. It is only after Bob announces

that he has performed all the measurements, that Alice makes string b public. This sequence of steps is essential. Alice and Bob now discard all bits in strings a and a' (where a' is the string representing Bob's measurement results) in all cases where Bob measured in a different basis from Alice. They are thus left with two identical strings, representing their private key.

A last step to be carried out in the protocol ensures the security of the transmission, determining whether or not an eavesdropper, aptly named Eve, managed to intercept their message. Due to basic postulates of quantum mechanics, if Eve observes the qubits, she will inevitably disturb their state. One other option for Eve would be to intercept the qubits from Alice, make a perfect copy of each one, then send them, in their original state, to Bob. However this is impossible due to the no-cloning theorem [55].

On average, Alice and Bob would choose a different basis 50% of the time. Because an eavesdropper would have the same probability of getting Alice's choices of bases wrong, if Bob observes that the probability of a mismatch in a subset of the string of his measurement results, with Alice's encryption choices is around 25%, this would mean that Eve has intercepted the message and the privacy of the key has been compromised.

a. The EPR Protocol

An important point about the BB84 protocol [37] relates to the source of the private key. Let Alice and Bob share n entangled states

$$|\psi\rangle = \frac{1}{\sqrt{2}}(|00\rangle + |11\rangle), \tag{31}$$

which have either been prepared by one of the parties and then half of each pair has been distributed to the other, or all pairs have been prepared by a third party and distributed to the two experimenters.

After using a Bell-type inequality to certify that the states are still entangled, they can be used for key distribution. The procedure would go like this

- Alice generates a classical string of bits b, and according to each value of the bits in this string, she measures her half of the EPR pairs, into either the Z or the X basis, obtaining a string a.
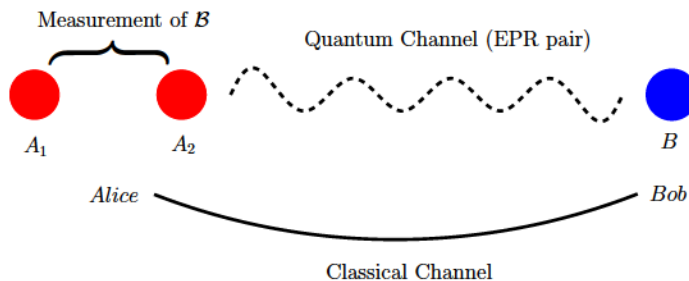
13

FIG. 4: Scheme of the quantum teleportation protocol.

- Bob does the same on his side of the EPR pair, obtaining a string a', by randomly choosing his measurement bases according to the values of a string of bits b'.

- Both experimenters communicate the values of b and b' and remove all instances in a and a', for which $b_k \neq b'_k$.

- The private key is represented by the common resulting string.

What is interesting here is that this key is only generated after both Alice and Bob perform their measurements on the EPR pairs, such that one cannot say the private key originated from one of the two parties.

2. Quantum Teleportation

A second application of entanglement we describe here is a procedure aptly named quantum teleportation. The purpose of this technique is the transmission of a previously unknown qubit state between two experimenters. The setup is as follows: two experimenters, Alice and Bob, share an entangled EPR pair and a classical communications channel. Alice must send the state of a third particle, in her possession, to Bob. As reference, see Ref [1] and [37], here we will mostly follow the former.

As previously mentioned, Alice and Bob share an EPR pair, denoted here as being comprised of the particles A_2 and B (see Fig.4). They are in the entangled state

$$|\psi_{A_2B}\rangle = \frac{1}{\sqrt{2}}(|0\rangle_{A_2}|1\rangle_B + |1\rangle_{A_2}|0\rangle_B).\tag{32}$$

Alice performs on particles A_1 and A_2 a measurement of the operator

14

$$\mathcal{B} = \sigma_1 \cdot \vec{a}(\sigma_2 \cdot \vec{b} + \sigma_2 \cdot \vec{b'}) + \sigma_1 \cdot \vec{a'}(\sigma_2 \cdot \vec{b} - \sigma_2 \cdot \vec{b'}), \tag{33}$$

which is nothing more than the CHSH inequality in operator form. The eigenbasis of $\mathcal{B}$ is the Bell basis,

$$
\begin{aligned}
|\psi^-\rangle &= \frac{1}{\sqrt{2}}(|0\rangle\,|1\rangle - |1\rangle\,|0\rangle), \\
|\psi^+\rangle &= \frac{1}{\sqrt{2}}(|0\rangle\,|1\rangle + |1\rangle\,|0\rangle), \\
|\phi^-\rangle &= \frac{1}{\sqrt{2}}(|0\rangle\,|0\rangle - |1\rangle\,|1\rangle), \\
|\phi^+\rangle &= \frac{1}{\sqrt{2}}(|0\rangle\,|0\rangle + |1\rangle\,|1\rangle).
\end{aligned}
\tag{34}
$$

Consider now that the state of particle A_1, which Alice intends to transmit to Bob, is

$$|A_1\rangle = a\,|0\rangle + a'\,|1\rangle. \tag{35}$$

We can write the total three-particle state in the form

$$
\begin{aligned}
|\psi_{AB}\rangle =&\frac{a}{\sqrt{2}}(|0\rangle_{A_1}|0\rangle_{A_2}|1\rangle_B - |0\rangle_{A_1}|1\rangle_{A_2}|0\rangle_B) \\
&+ \frac{a'}{\sqrt{2}}(|1\rangle_{A_1}|0\rangle_{A_2}|1\rangle_B - |1\rangle_{A_1}|1\rangle_{A_2}|0\rangle_B).
\end{aligned}
\tag{36}
$$

This can be further rewritten in the Bell basis as

$$
\begin{aligned}
|\psi_{AB}\rangle =&\frac{1}{\sqrt{2}}\big[\,|\psi^-\rangle_{A_1A_2}(-a\,|0\rangle_B - a'\,|1\rangle_B) \\
&+ |\psi^+\rangle_{A_1A_2}(-a\,|0\rangle_B + a'\,|1\rangle_B) \\
&+ |\phi^-\rangle_{A_1A_2}(a\,|1\rangle_B + a'\,|0\rangle_B) \\
&+ |\phi^+\rangle_{A_1A_2}(a\,|1\rangle_B - a'\,|0\rangle_B)\big].
\end{aligned}
\tag{37}
$$

After performing her Bell measurements on particles A_1 and A_2, Alice ends up with one of the four possible Bell states, while Bob obtains the corresponding pure state. Now, Alice must use a classical channel to inform Bob of which of the four states she obtained. Then, in order to recover the state $|A_1\rangle$, Bob has to perform one of the following unitary operations on

his state: $U_1 = -\mathbb{1}$, $U_2 = -\sigma_Z$, $U_3 = \sigma_X$ and $U_4 = -\sigma_X\sigma_Z$, depending on the state obtained by Alice.

There are two important remarks here. First, quantum teleportation does not allow for faster-than-light communication, since the two parties require a classical channel for the scheme to work. Indeed it can be quite easily shown (see. Ref.[37] section 2.4.3) that, in the absence of a classical channel, no information can be transmitted.

The second remark relates to the fact that it might seem the scheme produces a copy of the previously unknown state of particle A_1. If this were true, it would go against the predictions of the no-cloning theorem [55], however, it does not. Upon performing the EPR measurement on particles A_1 and A_2, Alice destroys the state of particle A_1, which just gets projected onto one of the eigenstates of σ_z. Thus, no copy of the unknown state is actually produced.

H.   Open Quantum Systems

Every quantum system is in contact with some environment, and because of this, one needs to provide a way to describe time evolution, taking the environment (or reservoir) into account. Isolated systems evolve in time in a unitary fashion, a pure state will always be mapped to another pure state. For open systems, this is not the case. An initial pure state will evolve into a mixed state. In what follows, a brief presentation of open systems is given. For more detail, some useful references are [1, 10].

1.   Decoherence and Dephasing

Two phenomena appear when a quantum system is in contact with an environment (or reservoir): decoherence and dephasing. They both affect the off-diagonal terms of the system's density matrix. In the following, a simple example [1] will be given to illustrate the effects of the two phenomena.

Consider a system S in contact with its environment E. For simplicity, let S be a two-level system, described by a state vector of the form

$$|\psi\rangle = c_0 |0\rangle + c_1 |1\rangle. \tag{38}$$

16

The environment's state can be expanded in terms of an arbitrary basis

$$|\mathcal{E}\rangle = \sum_n a_n |e_n\rangle, \tag{39}$$

and the state of the total system $(S + E)$ is thus

$$|\phi\rangle = |\psi\rangle |\mathcal{E}\rangle. \tag{40}$$

After the interaction this separability will be lost and the total state will be of the form

$$|\phi'\rangle = c_0 |0\rangle |\mathcal{E}_0\rangle + c_1 |1\rangle |\mathcal{E}_1\rangle, \tag{41}$$

where $|\mathcal{E}_0\rangle, |\mathcal{E}_1\rangle$ are generally non-orthogonal states of the reservoir.

The density matrix corresponding to this state is then

$$\begin{aligned}\rho_{SR} =& |c_0|^2 |0\rangle \langle 0 | \mathcal{E}_0\rangle \langle \mathcal{E}_0| + |c_1|^2 |1\rangle \langle 1 | \mathcal{E}_1\rangle \langle \mathcal{E}_1| \\ &+ c_0 c_1^* |0\rangle \langle 1 | \mathcal{E}_0\rangle \langle \mathcal{E}_1| + c_1 c_0^* |1\rangle \langle 0 | \mathcal{E}_1\rangle \langle \mathcal{E}_0|,\end{aligned} \tag{42}$$

and one can calculate the reduced density matrix of S by tracing out the environment,

$$\rho_S = \begin{pmatrix} |c_0|^2 & c_0 c_1^* \langle \mathcal{E}_1 | \mathcal{E}_0\rangle \\ c_1 c_0^* \langle \mathcal{E}_0 | \mathcal{E}_1\rangle & |c_1|^2 \end{pmatrix} \tag{43}$$

The off-diagonal elements are thus reduced by a factor of $|\langle \mathcal{E}_1 | \mathcal{E}_0\rangle|$. The more $|\mathcal{E}_0\rangle$ and $|\mathcal{E}_1\rangle$ get closer to being orthogonal, the smaller the off-diagonal elements tend to become.

Due to the environment's random fluctuations, another phenomenon called dephasing manifests itself. For simplicity, resort again to the example from Ref. [1]. Suppose that, after interacting with the environment, the state of S can be written as

$$|\psi\rangle = c_0 |0\rangle + c_1 e^{i\phi} |1\rangle, \tag{44}$$

where ϕ is some random phase. In the case of large fluctuations, the off-diagonal terms once more tend to zero, this time due to the fact that $\langle e^{i\phi}\rangle = 0$.

2. Dynamics of Closed Systems

Before considering the time evolution of open quantum systems it is useful to quickly sketch the simpler situation, namely for closed (or isolated) quantum systems.

The evolution of a pure state is given by the Schrödinger equation (where we drop the $\hbar$ term for simplicity)

$$\frac{\partial}{\partial t} |\psi(t)\rangle = -iH(t) |\psi(t)\rangle , \tag{45}$$

with the formal solution

$$|\psi(t)\rangle = U(t, t_0) |\psi(t_0)\rangle , \tag{46}$$

The time evolution for a closed system is unitary and we can write the unitary time evolution operator in terms of the Hamiltonian as

$$U(t, t_0) = \overleftarrow{T} \exp[-i \int_{t_0}^{t} ds H(s)], \tag{47}$$

and $U^\dagger U = UU^\dagger = \mathbb{1}$. Here we have used the notation from Ref. [35]. The time-ordering operator $\overleftarrow{T}$ orders products of unitary operators in a time-dependent way, such that the operators containing the earliest times are to the right of the product (i.e. they act first on the state vector).

In the case of a time-independent Hamiltonian, one can write the unitary operator in a simplified way

$$U(t, t_0) = \exp[-iH(t - t_0)]. \tag{48}$$

For mixed states

$$\rho(t) = \sum_n p_n |\psi_n(t)\rangle \langle \psi_n(t)| , \tag{49}$$

time evolution is given by the Liouville-von Neumann equation

$$\frac{\partial}{\partial t} \rho(t) = -i[H(t), \rho(t)]. \tag{50}$$

3. Dynamics of Open Systems

Having reviewed the time evolution equations for closed systems, we want to extend this to the more general open system case. Open quantum systems consist of a system of interest (denoted so far as S) and an environment with which it is in contact (denoted as E). In general, the time evolution of S is not unitary and we will need to make a number of approximations to obtain a usable time evolution equation. We will follow the derivations of Ref. [35], but one should also consider Ref. [10, 45]

The total Hilbert space of the combined system $(S + E)$ is

$$\mathcal{H} = \mathcal{H}_S \otimes \mathcal{H}_{\mathcal{E}}, \tag{51}$$

so we will be concerned with finding an equation for the reduced state (the state of S), thus we trace out the environment

$$\rho_S(t) = \text{Tr}_E(\rho(t)), \tag{52}$$

where $\rho(t)$ is the global state. Such an equation will be known as a master equation, whose definition [45] we give in the following.

Definition I.9. *A master equation is a first order differential equation describing the time evolution of probabilities, of the form*

$$\frac{dP_k}{dt} = \sum_l [T_{kl}P_l - T_{lk}P_k], \tag{53}$$

for some discrete events $k \in \{1, ..., N\}$ and where $T_{kl} \geq 0$ are transition rates from event l to event k, and P_k are the corresponding probabilities for the transitions.

In what follows, the above events should be understood as as different possible states of S. We first go through a step-by-step derivation of a Markovian master equation and then provide a form, similar to the one in Def.I.9, which is far more useful to implement. Before that, however, we should point out an essential aspect of master equations, namely that they conserve total probability

$$\sum_k \frac{dP_k}{dt} = \sum_{kl} [T_{kl}P_l - T_{lk}P_k] = \sum_{kl} [T_{lk}P_k - T_{lk}P_k] = 0. \tag{54}$$

19

A detailed discussion of how the master equation is obtained [35] is useful due to the fact that some important simplifying assumptions are made in the process. These assumptions restrict the applicability of the equation and explicitly show that the time-evolution rule thus obtained is only an approximation (something which should be taken into account in later chapters).

The system-environment Hamiltonian can be split into three operators

$$H = H_S + H_E + H_I,\tag{55}$$

where H_I is the interaction Hamiltonian, the only part that involves both system and environment degrees of freedom. We also denote $H_0 = H_S + H_E$ and switch to the interaction picture

$$\tilde{H}_I(t) = e^{i(H_S+H_E)t} H_I e^{-i(H_S+H_E)t},\tag{56}$$

with $t_0 = 0$.

The combined system $S + E$ is closed, so it evolves according to Eq.(50),

$$\frac{\partial}{\partial t}\tilde{\rho}(t) = -i[\tilde{H}(t), \tilde{\rho}(t)].\tag{57}$$

All operators marked with a tilde are written in the interaction picture, by using the Eq.(56) transformation.

The formal solution of Eq.(57) is

$$\tilde{\rho}(t) = \rho(0) - i\int_0^t ds[\tilde{H}_I(s), \tilde{\rho}(s)],\tag{58}$$

which, together with Eq.(57), gives

$$\frac{\partial}{\partial t}\tilde{\rho}(t) = -i[\tilde{H}(t), \rho(0)] - \int_0^t ds[\tilde{H}_I(t), [\tilde{H}_I(s), \tilde{\rho}(s)]].\tag{59}$$

Since we are only interested in the dynamics of the system, we trace-out the environment

$$\frac{\partial}{\partial t}\tilde{\rho}_S(t) = -i\,\mathrm{Tr}_E[\tilde{H}(t), \rho(0)] - \int_0^t ds\,\mathrm{Tr}_E[\tilde{H}_I(t), [\tilde{H}_I(s), \tilde{\rho}(s)]].\tag{60}$$

At this point one must make a series of simplifying assumptions. First, assume that the interaction between S and E is turned on exactly at $t = 0$. This means that the initial density operator factorizes

$$\rho(0) = \rho_S \otimes \rho_E(0). \tag{61}$$

Second, the term $\text{Tr}_E[H_I(t), \rho(0)]$ can be set to zero. This in effect means that we can subtract a term $\text{Tr}_E[H_I(t), \rho_E(0)]$ from H_I and include it in H_S. The time evolution equation now becomes

$$\frac{\partial}{\partial t}\tilde{\rho}_S(t) = -\int_0^t ds\, \text{Tr}_E[\tilde{H}_I(t), [\tilde{H}_I(s), \tilde{\rho}(s)]]. \tag{62}$$

Now we use the Born approximation, this further assumes that the interactions described by H_I are weak, so ρ_E is time-independent

$$\rho_E = \rho_E(0). \tag{63}$$

The density operator thus factorizes at all times

$$\tilde{\rho}(t) \approx \tilde{\rho}_S(t)\rho_E, \tag{64}$$

and time evolution will now be given by

$$\frac{\partial}{\partial t}\tilde{\rho}_S(t) = -\int_0^t ds\, \text{Tr}_E[\tilde{H}_I(t), [\tilde{H}_I(s), \tilde{\rho}_S(s)\rho_E]]. \tag{65}$$

The evolution of $\tilde{\rho}_S(t)$ still depends on its past history, through the $\tilde{\rho}_S(s)$ term. For this reason, the last approximation to be made is the Markovian approximation, stating that the future behaviour of $\tilde{\rho}_S(t)$ will only depend on its current state, hence we replace $\rho_S(s) \longrightarrow \rho_S(t)$ and $s \longrightarrow t - \tau$. Extending the limits of integration to infinity (See Ref. [35]), we finally obtain

$$\frac{\partial}{\partial t}\tilde{\rho}_S(t) = -\int_0^{\inf} d\tau\, \text{Tr}_E[\tilde{H}_I(t), [\tilde{H}_I(t - \tau), \tilde{\rho}_S(t)\rho_E]], \tag{66}$$

written in the interaction picture.

This is a Markovian weak-coupling master equation that provides a good approximation for the time-evolution of the open quantum system. However, it is very cumbersome to work
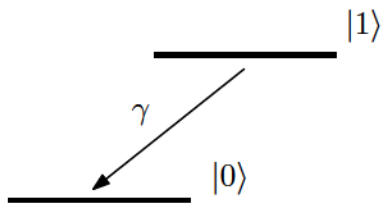
FIG. 5: A two level system with decay.

with so, in the next section, we provide an alternative form, known as a Lindblad form of the master equation and give a simple example of how it can be applied.

4. Lindblad Master Equation

In Ref. [9, 40], the authors provides simple derivations of the master equation in Lindblad form. Here, we only reproduce the result and go on to give a very simple example of how such an equation will be used in a later chapter, when we will apply it to neutral kaons and general decaying systems.

The Lindblad form of the master equation is

$$\frac{d}{dt}\rho(t) = -i[H, \rho(t)] - \sum_\alpha \frac{\gamma_\alpha}{2}(L^{\alpha\dagger}L^\alpha\rho(t) + \rho(t)L^{\alpha\dagger}L^\alpha - 2L^\alpha\rho(t)L^{\alpha\dagger}) \qquad (67)$$

or in the equivalent form

$$\frac{d}{dt}\rho(t) = -i[H, \rho(t)] - \sum_\alpha \gamma_\alpha(\frac{1}{2}\{L^{\alpha\dagger}L^\alpha\rho(t)\}_+ - L^\alpha\rho(t)L^{\alpha\dagger}), \qquad (68)$$

where $\{\cdot\}_+$ is the anticommutator and L^α are the Lindblad operators. In our case, the Lindblad operators will simply be jump operators, describing a transition between two quantum states.

Finally, we provide a simple example of a two-level system with decay and show how the Lindblad equation describes the decay process. Consider the two-level system in Fig. (5). We ignore any unitary time evolution and just focus on the decay from $|1\rangle$ to $|0\rangle$, with a decay rate γ.

The Lindblad equation would contain just the decay part

$$\frac{d}{dt}\rho(t) = \gamma(\frac{1}{2}\{\Lambda^\dagger\Lambda\rho(t)\}_+ - \Lambda\rho(t)\Lambda^\dagger), \tag{69}$$

where the Lindblad Λ operators are just jump operators between the two levels,

$$\Lambda = |0\rangle\langle 1|,$$
$$\Lambda^\dagger = |1\rangle\langle 0|. \tag{70}$$

I. Basic Notions of Experimental Quantum Optics

The last section of this introductory chapter will briefly present basic notions and techniques from the field of experimental quantum optics. We focus on the classical equations of motion for a trapping potential, laser cooling and internal state detection of a trapped ion. The main sources for this section are Ref.[20, 32, 52], to which we shall refer the interested reader for more detail.

1. Trapping Potential and Classical Equations of Motion

Due to Laplace's equation, one cannot trap a charged particle in three dimensions using only an electrostatic field, thus, following Ref.[32], we consider a quadrupolar potential which can be decomposed into an oscillating time-dependent part and a time-independent static part

$$\Phi(x, y, z, t) = \frac{U}{2}(\alpha x^2 + \beta y^2 + \gamma z^2) + \frac{\tilde{U}}{2}\cos(\omega_{rf}t)(\alpha' x^2 + \beta' y^2 + \gamma' z^2), \tag{71}$$

where ω_{rf} is the driving frequency. In order for this to fulfil the Laplace equation $\Delta\Phi = 0$, the following restrictions are imposed

$$\alpha + \beta + \gamma = 0,$$
$$\alpha' + \beta' + \gamma' = 0. \tag{72}$$

From these constraints, one observes that such a potential can only trap charges dynamically, by giving the trapped particles a quasi-harmonic motion in all directions.

23

There are two possible choices in terms of spatial factors,

$$\alpha = \beta = \gamma = 0,$$
$$\alpha' + \beta' = -\gamma', \tag{73}$$

giving three-dimensional confinement in an oscillating field, or

$$-(\alpha + \beta) = \gamma > 0,$$
$$\alpha' = -\beta', \tag{74}$$

which results in dynamical confinement in the XY-plane and static potential confinement for positive charges in the Z direction (as used in linear traps [39]).

We now shortly discuss the classical equations of motion of a particle in a trapping potential $\Phi(x, y, z, t)$. Considering only motion in the X-direction, the equation of motion becomes

$$\ddot{x} = -\frac{Z|e|}{m} \frac{\partial \Phi}{\partial x}$$
$$= -\frac{Z|e|}{m} [U\alpha + \tilde{U} \cos(\omega_{rf}t)\alpha']x, \tag{75}$$

which can be written as a Mathieu differential equation

$$\frac{d^2x}{d\xi^2} + [a_x - 2q_x \cos(2\xi)]x = 0 \tag{76}$$

using the substitutions

$$\xi = \frac{\omega_{rf}t}{2}, \qquad a_x = \frac{4Z|e|U\alpha}{m\omega_{rf}^2}, \qquad q_x = \frac{2Z|e|\tilde{U}\alpha'}{m\omega_{rf}^2} \tag{77}$$

The general form of the solutions is

$$x(2\xi) = Ae^{i\beta_x\xi} \sum_{m=-\infty}^{\infty} C_{2m}e^{i2m\xi} + Be^{-i\beta_x\xi} \sum_{m=-\infty}^{\infty} C_{2m}e^{-i2m\xi}, \tag{78}$$

here β_x and C_{2m} depend on a_x and q_x only.

One can now perform a lowest order approximation, by setting $C_{\pm 4} = 0$ and the condition that $A = B$. This leads to a simplified form of β_x
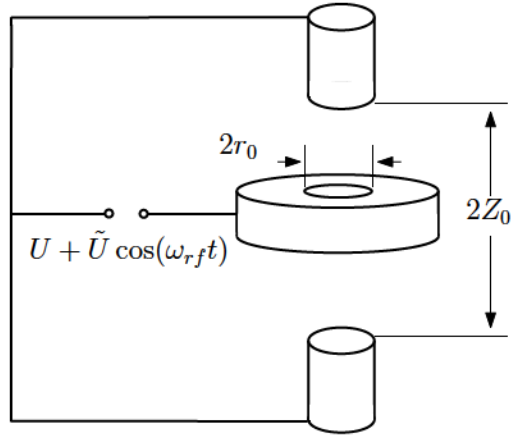
FIG. 6: Cylindrically-symmetric RF trap.

$$\beta_x = \sqrt{a_x + \frac{q_x^2}{2}}, \tag{79}$$

and of the particle trajectory

$$x(t) = 2AC_0 \cos\left(\beta_x \frac{\omega_{rf}}{2}t\right)\left[1 - \frac{q_x}{2}\cos(\omega_{rf}t)\right]. \tag{80}$$

The quantum mechanical description of the dynamics of charged particles in ion traps is somewhat more involved, so the reader is referred to Ref.[32] for that and also a more detailed treatment on classical motion and trap stability.

In Fig.6 the schematic of a cylindrically-symmetric RF trap is presented, with

$$a_z = -2a_x = -2a_y, \tag{81}$$
$$q_z = -2q_x = -2q_y,$$

and the requirements that $\alpha = \alpha' = \beta = \beta' = -2\gamma = -2\gamma'$ and also $\alpha = \frac{2}{r_0^2 + 2z_0^2}$.

Another possibility is to design a linear RF trap with

$$q_z = \gamma' = 0, \tag{82}$$
$$q_y = -q_x,$$

initially proposed by W. Paul [39]. This type of trap is more useful for manipulating individual ions with lasers.

25

As previously described, the motion of the trapped ion is composed of axial and transverse motion, with respect to the axis of the linear trap, with typical transverse frequencies being three to four times larger than the axial. In what follows, we focus exclusively on axial motion, for simplicity.

After the ion has been trapped, the next step is removing its vibrational energy, a process known as cooling.

2. Laser Cooling

Following Ref.[52], we describe here a cooling procedure known as side band cooling. Consider an atomic two-level system, a ground state $|g\rangle$ and an excited state $|e\rangle$, coupled to external lasers that drive a two-photon transition between them.

The Hamiltonian is, in this case

$$H = \hbar\nu a^\dagger a + \hbar\omega_A \sigma_z + \frac{\hbar\Omega}{2}(\sigma_- e^{i(\omega_L t - k_L q)} + \sigma_+ e^{-i(\omega_L t - k_L q)}), \tag{83}$$

where q is an operator representing the ion's displacement from its equilibrium position, ν is the trap frequency, Ω is the Rabi frequency of the transition, ω_A represents the atomic transition frequency while ω_L and k_L are the laser's frequency and wave number. The sigma matrices are given by

$$\begin{aligned} \sigma_- &= \frac{1}{2}(\sigma_x + i\sigma_y), \\ \sigma_+ &= \frac{1}{2}(\sigma_x - i\sigma_y), \end{aligned} \tag{84}$$

The key point here is the careful use of relations between the three frequencies ν, ω_A and ω_L.

We rewrite the position operator as

$$q = \left(\frac{\hbar}{2m\nu}\right)^{\frac{1}{2}}(a + a^\dagger), \tag{85}$$

and also define the Lamb-Dicke parameter

$$\eta = k_L \left(\frac{\hbar}{2m\nu}\right)^{\frac{1}{2}} = \frac{2\pi\Delta x_{rms}}{\lambda_L}, \tag{86}$$

with the root-mean-square (r.m.s.) position fluctuations given by Δx_{rms}.

By switching to the interaction picture, using

$$U_0(t) = e^{-i\nu a^\dagger a t - i\omega_A \sigma_z t},\tag{87}$$

one gets an interaction Hamiltonian of the form

$$H_I(t) = \frac{\hbar\Omega}{2}\left(\sigma_- e^{-i\eta(a e^{-i\nu t} + a^\dagger e^{i\nu t})} e^{-i(\omega_A - \omega_L)t} + h.c.\right)\tag{88}$$

This expression needs to be simplified, so we consider only small η, typically $\eta < 1$ and expand $H_I(t)$ in terms of this parameter. This, however, leads to a complicated expression and it is not the purpose of the current section to provide an in depth treatment of experimental methods. The interested reader can find the detailed derivation in Ref.[52]. Tuning $\delta = \omega - \omega_L$, such that it becomes an integer multiple of the trap frequency ν, one obtains three situations:

- carrier excitation, when $\delta = 0$

$$H_c = \hbar\Omega(1 - \eta^2 a^\dagger a)\sigma_x,\tag{89}$$

with $\sigma_x = \frac{1}{2}(\sigma_- + \sigma_+)$.

- first red sideband excitation, when $\delta = \nu$ (such that $\omega_L = \omega_A - \nu$)

$$H_r = i\frac{\hbar\eta\Omega}{2}(a\sigma_+ - a^\dagger\sigma_-).\tag{90}$$

- first blue sideband excitation, when $\delta = -\nu$ (such that $\omega_L = \omega_A + \nu$)

$$H_b = i\frac{\hbar\eta\Omega}{2}(a^\dagger\sigma_+ - a\sigma_-).\tag{91}$$

While in the case of the first red sideband excitation we have a process involving the absorption of a trap phonon, as well as a laser photon, in the case of the first blue sideband excitation, a phonon is emitted. If the ion is in the excited state $|e\rangle$ and it spontaneously decays to the ground state, tuning to the first red sideband, we obtain cycles of excitation and emission that remove one phonon per cycle, cooling the vibrational degree of freedom.
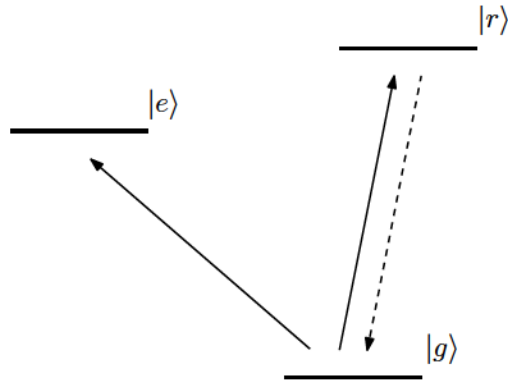
27

FIG. 7: Three level system used for electron shelving.

3. Reading the Internal State

After trapping and cooling the ion, the last step to be discussed here is the detection of its internal states. This is usually performed by laser-induced fluorescence. In this process, one ion can scatter large numbers of photons, some of which can be picked up by a detector (such as a CCD camera or a photon-multiplier). Because the spatial extension of the ion's wave function is smaller than the wavelength of the fluorescent light, single ions will show up as bright dots.

One detection procedure is the so-called electron shelving method. Consider adding an extra level $|r\rangle$ to the previously introduced two-level system, as in Fig.7. Further assume that [32] the transitions $|g\rangle \leftrightarrow |e\rangle$ and $|g\rangle \leftrightarrow |r\rangle$ can be independently driven, and that the lifetime of $|r\rangle$ is much shorter than the lifetimes of the other two levels. Thus, the transition $|g\rangle \leftrightarrow |r\rangle$ can be strongly driven and a large number of scattered photons if the initial interaction with the laser field prepared the atom in the state $|r\rangle$. On the other hand, if the initial state of the atom, after being excited by the laser, is $|e\rangle$, no photons will be scattered.

II.   Neutral Kaons

In the first half of this thesis we will be presenting our results [38], as well as previous ones, regarding the study of entanglement in systems of decaying particles. The testbed for this will be a system of electrically neutral mesons, called neutral k-mesons or neutral kaons for short.

Mesons are hadrons (composite particles made of quarks) composed of one quark and one antiquark, bound together by strong interaction. In particular, neutral kaons are composed of a down quark and a strange antiquark.

Historically, neutral kaons have been essential in providing an insight into the quark structure of hadrons and the theory of quark mixing, for which a Nobel Prize in Physics has been awarded in 2008, and in deepening our understanding on the matter-antimatter asymmetry in the universe. On this second subject, the violation of charge conjugation and parity (CP) symmetry was first observed experimentally in systems of neutral kaons by J.W. Cronin and V. L. Fitch [11], and brought the two the 1980 Nobel Prize in Physics.

As we shall see, neutral kaons exhibit two types of behaviour that give the experimenter a new possibility of performing Bell tests: a particle-antiparticle oscillation and decay. Before this, however, a more thorough description of the particles will be given.

Neutral kaons are pseudo-scalar mesons, even though their total spin is zero, they have odd parity, denoted by $J^P = 0^-$, compared to scalar mesons which have even parity $J^P = 0^+$. They are produced in particle-antiparticle pairs $(K^0 \bar{K}^0)$, either in electron-positron collisions (DAΦNE at Frascati) or proton-antiproton collisions (CPLEAR at CERN). For this reason, we must always treat neutral kaons as a two-particle system.

At time $t = 0$, the initial state function for the pair is

$$|\psi(t=0)\rangle = \frac{1}{\sqrt{2}}(|K^0\rangle|\bar{K}^0\rangle - |\bar{K}^0\rangle|K^0\rangle). \tag{92}$$

Time evolution will be treated in detail later on in this chapter, but first, we want to describe in more detail CP-symmetry and the Cronin-Fitch experiment.
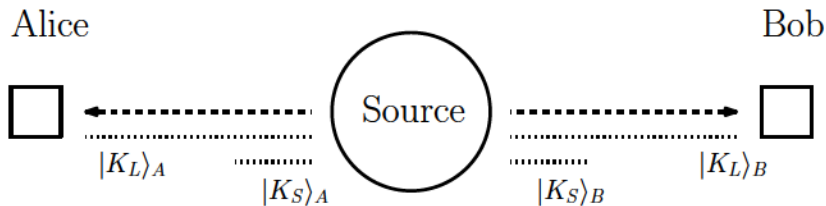
FIG. 8: Neutral kaon pair production. Beams of kaon-antikaon pairs propagate in opposite directions. The beams contain two different mass states, a short-lived state $|K_S\rangle$ and a long-lived state $|K_L\rangle$.

A.   CP-symmetry and its Violation

1.   Theoretical Remarks

As previously stated, neutral kaons are pseudoscalar particles hence they have odd (negative) intrinsic parity. They are produced in a standard collision setup (see Fig. 8) and propagate in opposite directions from the source. Due to a continuous oscillation between $|K^0\rangle$ and $|\bar{K}^0\rangle$, one must consider the two opposing beams of particles as containing both particles and antiparticles. The two particle beams can also be described in another basis, the lifetime basis, composed of a long-lived and short-lived state, $|K_L\rangle$ and $|K_S\rangle$, respectively. These two states can be experimentally distinguished by observing the dominant resulting decay products. The exact forms of $|K_L\rangle$ and $|K_S\rangle$ will be discussed later, for now it suffices to think of them as superpositions of $|K^0\rangle$ and $|\bar{K}^0\rangle$. One important aspect of the lifetime eigenstates is their vastly different lifetimes: $\tau_S = 8.95 \cdot 10^{-11}$s and $\tau_L = 5.11 \cdot 10^{-8}$s.

One feature of neutral kaons is a property called strangeness. In fact, for our purposes, we can consider strangeness as an operator whose eigenstates are the particle-antiparticle states themselves,

$$
\begin{aligned}
S\left|K^0\right\rangle &= (+1)\left|K^0\right\rangle, \\
S\left|\bar{K}^0\right\rangle &= (-1)\left|\bar{K}^0\right\rangle.
\end{aligned}
\tag{93}
$$

Having the notion of strangeness formally defined, we can look the operation that transforms one of the eigenstates of the strangeness operator into the other (or, in other words, that transforms a particle to its antiparticle). That operation is charge conjugation. However,

30

since we are interested in the violation of CP-symmetry, we couple the charge conjugation transformation with the parity transformation, and obtain the effects of the combined CP operator on the kaon states,

$$CP\left|K^0\right\rangle = (-1)\left|\bar{K}^0\right\rangle,$$
$$CP\left|\bar{K}^0\right\rangle = (-1)\left|K^0\right\rangle. \tag{94}$$

From this, one can now easily construct the eigenstates of the CP operator

$$\left|K_1^0\right\rangle = \frac{1}{\sqrt{2}}(\left|K^0\right\rangle - \left|\bar{K}^0\right\rangle),$$
$$\left|K_2^0\right\rangle = \frac{1}{\sqrt{2}}(\left|K^0\right\rangle + \left|\bar{K}^0\right\rangle), \tag{95}$$

such that

$$CP\left|K_1^0\right\rangle = (+1)\left|K_1^0\right\rangle,$$
$$CP\left|K_2^0\right\rangle = (-1)\left|K_2^0\right\rangle. \tag{96}$$

The violation of CP-symmetry is directly linked to the matter-antimatter imbalance in the universe; there are vastly more particles than antiparticles observed, and the reason for this is still not entirely understood.

Because CP-violation has been observed experimentally in the neutral kaon system, it follows that the system's Hamiltonian (whose eigenstates, as we've previously mentioned, are precisely $\left|K_L\right\rangle$ and $\left|K_S\right\rangle$) and the CP operator do not commute, hence they do not have common eigenstates.

The CP-violation parameter for kaons has an experimentally determined value of approximately $\epsilon = 10^{-3}$, so it is usual to write the short and long-lived states as

$$\left|K_S\right\rangle = \frac{1}{N}(p\left|K^0\right\rangle - q\left|\bar{K}^0\right\rangle),$$
$$\left|K_L\right\rangle = \frac{1}{N}(p\left|K^0\right\rangle + q\left|\bar{K}^0\right\rangle), \tag{97}$$

where $p = 1 + \epsilon$, $q = 1 - \epsilon$ and the normalization coefficient is $N^2 = |p|^2 + |q|^2$. By comparing Eq. (95) and Eq. (97), one can indeed observe that the slight difference between the two bases is given by the p and q coefficients, corresponding to the small, experimentally observed, ϵ

parameter. Also, it is straightforward to show that $|K_L\rangle$ and $|K_S\rangle$ are normalized but not orthogonal,

$$\langle K_L \,|\, K_S \rangle = \frac{1}{N^2}(|p|^2 - |q|^2) = \frac{|p|^2 - |q|^2}{|p|^2 + |q|^2}. \tag{98}$$

2. The Cronin and Fitch Experiment

The short and long-lived kaon states $|K_L\rangle$ and $|K_S\rangle$ have different decay modes. A state of π-particles (or pions) has parity

$$P = (-1)^n(-1)^L. \tag{99}$$

For spinless kaon decays $L = 0$ so

$$P\,|2\pi\rangle = +\,|2\pi\rangle\,, $$
$$P\,|3\pi\rangle = -\,|3\pi\rangle\,. \tag{100}$$

Because

$$C\,\big|n\pi^0\big\rangle = +\,\big|n\pi^0\big\rangle\,, \tag{101}$$

in the case of neutral pions, since they have no electromagnetic charge and

$$C\,\big|\pi^+\pi^-\big\rangle = +\,\big|\pi^+\pi^-\big\rangle\,, \tag{102}$$

due to charge cancellation in the case of positive and negatively charged pions, combinations of π^0 or π^0 and a pair of $\pi^+\pi^-$ do not change the value of C. If one thus assumes CP-symmetry to be conserved, the only allowed decay modes are (by combining the two C and P operations),

$$|K_S\rangle \longrightarrow |\pi\pi\rangle\,, $$
$$|K_L\rangle \longrightarrow |\pi\pi\pi\rangle\,. \tag{103}$$

The states $|K_L\rangle$ and $|K_S\rangle$ also have very different lifetimes,

Distance from the source to the detector ≈ 17.4 m.

$|K_L\rangle$
$|K_S\rangle$

S

Decay of $|K_S\rangle$ to 1/500 of original population.
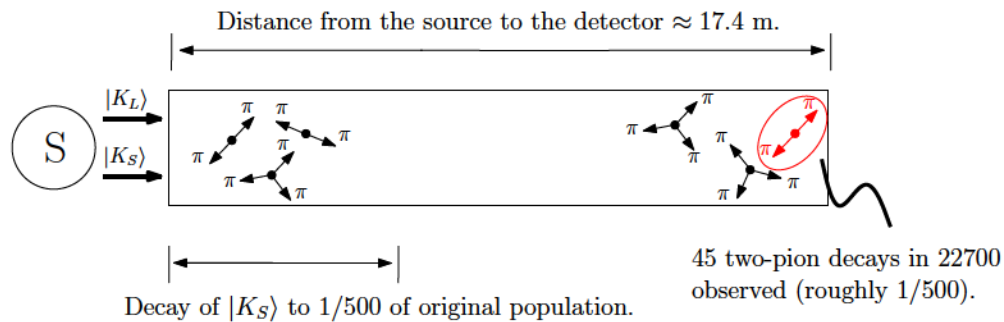
45 two-pion decays in 22700 observed (roughly 1/500).

FIG. 9: A schematic representation of the Cronin and Fitch experiment. Even with relativistic corrections, two-pion decays were observed at a rate of 1/500, at a greater distance than the one required for the sort-lived state to decay to the same extent. This picture has been reproduced from the one in Ref. [27].

$$\tau_{K_S} = 8.9 \cdot 10^{-11}s \qquad\qquad \tau_{K_L} = 5.2 \cdot 10^{-8}s, \qquad\qquad (104)$$

which would make it possible to distinguish between the two by looking at their decay products at a certain distance away from the source.

In 1964, Cronin and Fitch [11] had devised an experiment to test the conservation of CP-symmetry. A sketch of the experimental setup is provided in Fig. 9.

A particle beam of length $L = 17.4m$ contains both $|K_L\rangle$ and $|K_S\rangle$ states, coming from a source S. Taking into account relativistic corrections (see also Ref. [27]) and a particle travelling at a speed of $v = 0.98c$, the short-lived state would have decayed by a factor of one in five hundred of the initial population at roughly one meter from the source. This is also the distance at which one could expect two-pion events to occur with the same 1/500 frequency, since, if CP-symmetry is conserved, these events can only occur from the $|K_S\rangle$ state.

Experimentally, Cronin and Fitch observed 45 (± 9) 2π decays out of 22700, or approximately one in five hundred. These decay events, at $17.4m$ from the source could have only resulted from the long-lived state $|K_L\rangle$, a decay forbidden by CP-symmetry, hence the neutral kaon system violates this type of symmetry.

B. Time Evolution of the Neutral Kaon System

Neutral kaons display two types of behaviour that make them interesting to the study of entanglement: first there is the decay process, bringing with it the challenge of defining a qubit state within a more realistic representation of the actual quantum system as an open system; second, an intrinsic oscillation between particle and antiparticle states (called strangeness oscillation). This oscillation offers experimenters a new possibility of performing Bell tests, by having one of the parties wait for an additional time τ after the other party performed the measurement. This serves to give the particle measured at a later time an additional interval in which to oscillate, thus τ can serve as an "angle" for some spin-like quantity (which we will later define rigorously).

Before discussing Bell-tests on kaons, however, and the various available settings, we must derive in detail the time-dependent forms of $|K^0\rangle$ and $|\bar{K}^0\rangle$.

Since we are dealing with an open system, it is usual to split the Hamiltonian into a hermitian and an antihermitian part (see Ref.[4])

$$H = M - i\Gamma, \tag{105}$$

where H is called an effective Hamiltonian, M is the mass term (or mass matrix), responsible for the unitary time evolution, and Γ is the decay matrix. Both matrices are diagonal in the eigenbasis of H (represented by the two lifetime eigenstates $|K_S\rangle$ and $|K_L\rangle$), with the different masses, $m_{S/L}$ and decay rates $\Gamma_{S/L}$, of the short and long-lived states, as their elements.

With this, the eigenvalue equations of the Hamiltonian are

$$H|K_S\rangle = \lambda_S |K_S\rangle,$$
$$H|K_L\rangle = \lambda_L |K_L\rangle, \tag{106}$$

where the eigenvalue itself can be decomposed as $\lambda_{S/L} = m_{S/L} - \frac{i}{2}\Gamma_{S/L}$.

From the definition of $|K_S\rangle$ and $|K_L\rangle$,

$$|K_S\rangle = \frac{1}{N}(p|K^0\rangle - q|\bar{K}^0\rangle),$$
$$|K_L\rangle = \frac{1}{N}(p|K^0\rangle + q|\bar{K}^0\rangle), \tag{107}$$

one can extract $|K^0\rangle$ as

$$|K^0\rangle = \frac{N}{2p}(|K_S\rangle + |K_L\rangle). \tag{108}$$

In order to obtain a time-dependent form of $|K^0\rangle$, it suffices to use the eigenvalue equations (106) into (108), to obtain

$$
\begin{aligned}
\left|K^0(t)\right\rangle &= \frac{N}{2p}(e^{-i\lambda_S t}\left|K_S\right\rangle + e^{-i\lambda_L t}\left|K_L\right\rangle) \\
&= \frac{N}{2p}\left[e^{-i\lambda_S t}\frac{1}{N}(p\left|K^0\right\rangle - q\left|\bar{K}^0\right\rangle) + e^{-i\lambda_L t}\frac{1}{N}(p\left|K^0\right\rangle + q\left|\bar{K}^0\right\rangle)\right] \\
&= \frac{1}{p}\left[\frac{p}{2}(e^{-i\lambda_S t} + e^{-i\lambda_L t})\left|K^0\right\rangle + \frac{q}{2}(-e^{-i\lambda_S t} + e^{-i\lambda_L t})\left|\bar{K}^0\right\rangle\right].
\end{aligned}
\tag{109}
$$

The above expression can be simplified by introducing the notation

$$
\begin{aligned}
g_+(t) &= \frac{1}{2}(e^{-i\lambda_S t} + e^{-i\lambda_L t}), \\
g_-(t) &= \frac{1}{2}(-e^{-i\lambda_S t} + e^{-i\lambda_L t}),
\end{aligned}
\tag{110}
$$

such that Eq.(109) becomes

$$\left|K^0(t)\right\rangle = g_+(t)\left|K^0\right\rangle + \frac{q}{p}g_-(t)\left|\bar{K}^0\right\rangle. \tag{111}$$

Following the same line of reasoning, one can find the time-dependent antiparticle state

$$\left|\bar{K}^0(t)\right\rangle = \frac{p}{q}g_-(t)\left|K^0\right\rangle + g_+(t)\left|\bar{K}^0\right\rangle. \tag{112}$$

In a typical Bell-setup, the two parties share the time-dependent state

$$|\phi(t)\rangle = \frac{1}{\sqrt{2}}(\left|K^0(t)\right\rangle\left|\bar{K}^0(t)\right\rangle - \left|\bar{K}^0(t)\right\rangle\left|K^0(t)\right\rangle), \tag{113}$$

and if Alice would have performed a measurement and would have found her particle to be in a $|K^0\rangle$ state, Bob's particle, at that moment, would be in the state $|\bar{K}^0\rangle$. This is the point where neutral kaons allow the experimenter to alter the traditional Bell test, namely Bob can wait for an additional time τ, and there is a non-zero probability that, when measuring, he also obtains a $|K^0\rangle$ state. We shall use this when deriving the effective formalism for neutral

kaons, by defining a quasi-spin in terms of $|K^0\rangle$ and $|\bar{K}^0\rangle$ (where these two states would play the role of spin $+\frac{1}{2}$ or $-\frac{1}{2}$, in the case of a spin-1/2 particle).

One last derivation we carry out in detail is for finding time-dependent expressions for possible measurements in the strangeness eigenbasis ($|K^0\rangle$ / $|\bar{K}^0\rangle$).

First, consider the probability at time t that a measurement performed on a single neutral kaon, initially in a state $|K^0\rangle$, would yield the result $|K^0\rangle$. This is formally given by

$$P_{K^0K^0} = |\langle K^0 | K^0(t)\rangle|^2 = |g_+(t)|^2, \tag{114}$$

where the last term results directly from Eq.(111). Elaborating on this expression

$$
\begin{aligned}
|g_+(t)|^2 &= \frac{1}{4}|e^{-i\lambda_S t} + e^{-i\lambda_L t}|^2 \\
&= \frac{1}{4}|e^{-i(m_S - \frac{i}{2}\Gamma_S)t} + e^{-i(m_S - \frac{i}{2}\Gamma_L)t}|^2 \\
&= \frac{1}{4}\left[e^{-\Gamma_S t} + e^{-\Gamma_L t} + 2e^{-\frac{\Gamma_S + \Gamma_L}{2}t}\cos(m_L - m_S)t\right] \\
&= \frac{1}{4}\left[e^{-\Gamma_S t} + e^{-\Gamma_L t} + 2e^{-\Gamma t}\cos(\Delta m)t\right],
\end{aligned}
\tag{115}
$$

with $\Gamma = \frac{\Gamma_S + \Gamma_L}{2}$ and $\Delta m = m_L - m_S$.

Once more, by following similar reasoning, one can find the remaining expressions which we list below

$$
\begin{aligned}
P_{\bar{K}^0K^0} &= |\langle \bar{K}^0 | K^0(t)\rangle|^2 = \frac{1}{4}\frac{|q|^2}{|p|^2}\left[e^{-\Gamma_S t} + e^{-\Gamma_L t} - 2e^{-\Gamma t}\cos(\Delta m)t\right] \\
P_{K^0\bar{K}^0} &= |\langle K^0 | \bar{K}^0(t)\rangle|^2 = \frac{1}{4}\frac{|p|^2}{|q|^2}\left[e^{-\Gamma_S t} + e^{-\Gamma_L t} - 2e^{-\Gamma t}\cos(\Delta m)t\right] \\
P_{\bar{K}^0\bar{K}^0} &= |\langle \bar{K}^0 | \bar{K}^0(t)\rangle|^2 = \frac{1}{4}\left[e^{-\Gamma_S t} + e^{-\Gamma_L t} + 2e^{-\Gamma t}\cos(\Delta m)t\right]
\end{aligned}
\tag{116}
$$

C. Bell Inequalities and Neutral Kaons

Having obtained the time evolution equations for the neutral kaon system, we can now discuss possible implementations of Bell tests. It can be tempting to treat neutral kaons (or the similarly behaving B-mesons) in analogy to photons [22, 23], however there are some important shortcomings to such an approach. In what follows, we consider a parallel treatment of photons within optical fibers and kaons.

Considering a photon's linear and circular polarization states, one can define two bases (see. Ref.[22]): $\{|L\rangle, |R\rangle\}$, corresponding to the circular left and right polarization states and $\{|H\rangle, |V\rangle\}$, corresponding to the horizontal and vertical polarizations, respectively. The transformation between the two bases is given by

$$
\begin{aligned}
|L\rangle &= \frac{1}{\sqrt{2}}(|V\rangle + |H\rangle), \\
|R\rangle &= \frac{1}{\sqrt{2}}(|V\rangle - |H\rangle),
\end{aligned}
\tag{117}
$$

and

$$
\begin{aligned}
|V\rangle &= \frac{1}{\sqrt{2}}(|L\rangle + |R\rangle), \\
|H\rangle &= \frac{1}{\sqrt{2}}(|L\rangle - |R\rangle).
\end{aligned}
\tag{118}
$$

Comparing this with Eq.(95), one can identify the photon polarization states with the strangeness eigenstates $|K^0\rangle$ and $|\bar{K}^0\rangle$ and the CP-eigenstates $|K_1^0\rangle$ and $|K_2^0\rangle$. However, the CP-violation phenomenon cannot be ignored, such that, upon performing a measurement, the choice is between the strangeness eigenstates and the eigenstates of the Hamiltonian, Eq.(97), thus a first case of dissimilarity between the two systems.

What is possible, however, is to simulate decay and strangeness oscillations with photons. In Ref.[22], the authors describe the possibility of using birefringence and polarization-dependent loss as analogous phenomena. Birefringence determines fast and slow polarization modes which can be identified with $|V\rangle$ and $|H\rangle$, respectively. Any polarization state can be represented by a point on the Bloch sphere (in quantum optics sometimes referred to as the Poincaré sphere). The effect of birefringence on the corresponding Bloch vector $\vec{m}(z)$, at position z along the optical fiber, is that it causes it to rotate around a birefringent axis $\vec{\beta}$. If one looks at the time evolution of the pure polarization state, for a fixed wavelength, the following occurs

$$
|\vec{m}(z)\rangle = e^{-i\vec{\beta}\vec{\sigma}/2(z-z_0)} |\vec{m}(z_0)\rangle .
\tag{119}
$$

The vector $\vec{\sigma}$ is the Pauli vector, having the Pauli matrices as components and $U(\alpha) = e^{-i\vec{\beta}\vec{\sigma}/2}$ is the unitary operator corresponding to the rotation. If the experiment is performed with

σ Eigenvector	Photons	Neutral Kaons
$\lvert x+\rangle$	$\lvert V\rangle$	$\lvert K^0\rangle$
$\lvert x-\rangle$	$\lvert H\rangle$	$\lvert \bar{K}^0\rangle$
$\lvert z+\rangle$	$\lvert R\rangle$	$\lvert K_1^0\rangle\,(\approx \lvert K_S\rangle)$
$\lvert z-\rangle$	$\lvert L\rangle$	$\lvert K_2^0\rangle\,(\approx \lvert K_L\rangle)$

TABLE II: Correspondence between relevant kaon states, photon polarization states and the eigenvectors of the σ_x and σ_z Pauli matrices.

an initial singlet state, after observing one of the photons, the experimenter can wait an additional time before performing the second measurement and, due to the birefringence-caused rotation, allow the second photon's polarization to further rotate. In this way, the polarization correlation is reduced and the system has a similar property to the neutral kaon system's natural strangeness oscillation.

In order to also add a decay property to the photon system, we can introduce a polarizer that would attenuate the two polarization states differently. Considering two orthogonal polarization states $\lvert P_+\rangle$ and $\lvert P_-\rangle$, the transmission coefficients T_{max} and T_{min}, for the two states would differ, corresponding to the Γ_S and Γ_L case for kaons.

The testing of Bell-type inequalities within meson systems (in our case neutral K-mesons) requires the taking into consideration of two important aspects [5]:

- The two observers have to be able to perform *active measurements* on their paricles.

- Decay products cannot be ignored.

The first requirement is essential for enforcing the locality condition. Alice must be able to freely choose between two different bases A and A', and Bob, between B and B'. The argument is that (see Ref.[5]) if Alice had chosen, at the very last moment, to measure A instead of A', this choice would not modify the outcome of Bob's measurement.

In the case of neutral kaons, there are two types of measurements that one can carry out (For a detailed discussion, see Ref.[8]). Active measurements are experimentally made possible by introducing a dense piece of matter in the flight path of the kaons, at a flight time τ. The kaon's interaction with the matter corresponds to a projection of the initial

time-dependent state of Eq. (111)-(112), onto the lifetime or strangeness eigenbasis. By carefully selecting the flight time τ, from the source to the piece of mater, the experimenter can perform a strangeness or lifetime measurement at different times.

Passive measurements require the measurement of a time-dependent decay rate $\Gamma(f, \tau)$, which represents the number of decays into mode f, in the time interval τ and $\tau + d\tau$. These measurements are not useful for testing Bell inequalities, since they do not provide a way for the experimenter to choose the basis into which the measurement is done, there is, essentially, no way of forcing the particle to decay.

The second requirement is due to the unstable nature of mesons. The complete time evolution of a general meson system can be written in the form

$$|M_{1,2}(t)\rangle = e^{i\lambda_{1,2}t} |M_{1,2}\rangle + |\Omega_{1,2}(t)\rangle \,, \tag{120}$$

in terms of the eigenvectors of the "effective mass" non-Hermitian Hamiltonian. The resulting decay product state $|\Omega_{1,2}(t)\rangle$ brings its contribution by providing an extra outcome as opposed to the case of stable particles. If the measurement is performed in the strangeness eigenbasis, the results can be "$|K^0\rangle$" , "$|\bar{K}^0\rangle$" or "$|\Omega\rangle$". The last situation corresponds to the case when the observed particle has decayed prior to the measurement.

In the next chapter, we will discuss an existing effective operator formalism that manages to overcome these restrictions by switching to the Heisenberg picture and constructing an operator that contains both the characteristic time evolution of the system (decay and strangeness oscillation) and the measurement settings corresponding to a measurement of strangeness or lifetime on a single particle. We will then provide our generalization of this effective formalism to arbitrary decaying systems, retaining neutral kaons as a special case, and provide possible experimental implementations using trapped ions.

III. Effective Formalism

1. Special Effective Formalism

In Ref. [18], the authors present an effective formalism, constructed specifically for neutral kaons, that aims to go around the previously discussed impediments. We will develop this formalism here, in detail, and then proceed to deriving our generalization to one applicable to other decaying systems. We shall also prove that our general formalism reproduces the results of the special effective formalism, in the case of kaons.

The main difference between the way Bell inequalities have usually been tested with kaons (by analogy with photons and other stable systems) and the effective formalism, is the question that is being asked. In the standard Bell scenario, a dichotomic observable is measured (for example the spin of a spin$-\frac{1}{2}$ particle or the polarization of a photon) and the corresponding question to this would be "Is the system in a $|\uparrow\rangle$ or in a $|\downarrow\rangle$ state ?" (or two orthogonal polarization states, for photons). The issue here is that this type of question leaves no room for the decay products. While this may suffice for the above mentioned stable systems, it does not suffice for kaons.

The question asked within the effective formalism is "Is the system in a $|\uparrow\rangle$ state or not?". By "or not" we assume that it does not matter if the system finds itself in the corresponding orthogonal state or if it has already decayed. To translate this for our particular case, the question for a strangeness measurement is: "Is the system in a $|\bar{K}^0\rangle$ state or not?". There is nothing special here about $|\bar{K}^0\rangle$, we could have chosen $|K^0\rangle$ just as well.

a. Quasi-spin and Expectation Values

In order to draw a parallel with spin, a pseudo-quantity called *quasi spin* is introduced, whose direction is given by

$$|k_n\rangle = \cos \frac{\alpha_n}{2} |K_S\rangle + \sin \frac{\alpha_n}{2} e^{i\phi_n} |K_L\rangle , \tag{121}$$

in terms of the lifetime eigenstates. This can be transformed to the strangeness eigenbasis by using Eq.(97). Care must be taken here when choosing the appropriate α and ϕ angles.

While in the case of spin, it does make sense to choose arbitrary directions, for kaons it does not. The choices or quasi-spin directions are limited to the strangeness $\left|\bar{K}^0\right\rangle / \left|K^0\right\rangle$ and lifetime $\left|K_S\right\rangle / \left|K_L\right\rangle$ eigenstates.

Now, by taking advantage of the fact that probabilities must add up to one

$$P(\bar{K}^0) + P(K^0) + P(\Omega) = 1, \tag{122}$$

this can be rewritten as

$$\begin{aligned} P(Yes) &= P(\bar{K}^0), \\ P(No) &= 1 - P(K^0) - P(\Omega), \end{aligned} \tag{123}$$

where "Yes" and "No" are precisely the answers to the relevant question: "Is the system in a $\left|\bar{K}^0\right\rangle$ state or not?", and $P(\Omega)$ is the probability that the particle has decayed prior to being measured. Furthermore, now we clearly have $P(Yes) + P(No) = 1$.

Using the quasi-spin form of Eq. (121), the expectation value can now be written based on these two probabilities

$$\begin{aligned} E(k_n, t_n) &= P(Y : k_n, t_n) - P(N : k_n, t_n) \\ &= 2P(Y : k_n, t_n) - 1, \end{aligned} \tag{124}$$

the index n showing that this corresponds to one of the measurement settings of Alice and Bob, at time t_n. The time-dependent density matrix of the entire system can be described in terms of its surviving and decayed components

$$\rho(t_n) = \begin{pmatrix} \rho_{ss} & \rho_{sf} \\ \rho_{fs} & \rho_{ff} \end{pmatrix} \tag{125}$$

the subscript s labelling surviving components and f (for final) labelling decayed ones. The probability for obtaining the desired direction of the quasi-spin is then just a projection of the surviving kaon states onto $\left|k_n\right\rangle$,

$$P(Y : k_n, t_n) = Tr\left[\begin{pmatrix} \left|k_n\right\rangle \left\langle k_n\right| & 0 \\ 0 & 0 \end{pmatrix} \rho(t_n) \right] = \left\langle k_n\right| \rho_{ss}(t_n) \left|k_n\right\rangle. \tag{126}$$

This can be further expanded in the lifetime eigenbasis

$$\langle k_n | \rho_{ss}(t_n) | k_n \rangle = \cos^2 \frac{\alpha_n}{2} \langle k_S | \rho_{ss}(t_n) | k_S \rangle + \sin^2 \frac{\alpha_n}{2} \langle k_L | \rho_{ss}(t_n) | k_L \rangle$$
$$+ \cos \frac{\alpha_n}{2} \sin \frac{\alpha_n}{2} e^{i\phi_n} \langle k_S | \rho_{ss}(t_n) | k_L \rangle + \cos \frac{\alpha_n}{2} \sin \frac{\alpha_n}{2} e^{-i\phi_n} \langle k_L | \rho_{ss}(t_n) | k_S \rangle$$
$$= \rho_{SS} \cos^2 \frac{\alpha_n}{2} e^{-\Gamma_S t} + \rho_{LL} \sin^2 \frac{\alpha_n}{2} e^{-\Gamma_L t} + \rho_{SL} \cos \frac{\alpha_n}{2} \sin \frac{\alpha_n}{2} e^{i\phi_n} e^{-i\Delta m t - \Gamma t}$$
$$+ \rho_{LS} \cos \frac{\alpha_n}{2} \sin \frac{\alpha_n}{2} e^{-i\phi_n} e^{i\Delta m t - \Gamma t}.$$

Here, ρ_{SS}, ρ_{SL}, ρ_{LS}, ρ_{LL}, represent the elements of the density matrix in the lifetime eigenbasis $\{ |K_S\rangle, |K_L\rangle \}$ (not to be confused with $|\rho_{ss}\rangle$, the component of surviving particles). A rescaling $\Delta m = 1$ such that $\Gamma_i = \frac{\Gamma_i}{\Delta m}$ will be used, and the final form of the probability to obtain the desired direction for the quasi-spin, at time t_n, in terms of the lifetime elements of ρ is

$$P(Yes : k_n, t_n) = \rho_{SS} \cos^2 \frac{\alpha_n}{2} e^{-\Gamma_S t_n} + \rho_{LL} \sin^2 \frac{\alpha_n}{2} e^{-\Gamma_L t_n}$$
$$+ \rho_{SL} \cos \frac{\alpha_n}{2} \sin \frac{\alpha_n}{2} e^{i(\phi_n - t_n)} e^{-\Gamma t_n} \tag{127}$$
$$+ \rho_{LS} \cos \frac{\alpha_n}{2} \sin \frac{\alpha_n}{2} e^{-(i\phi_n - t_n)} e^{\Gamma t_n},$$

where $\Gamma = \frac{\Gamma_S + \Gamma_L}{2}$.

b. Effective Operator Matrix Form

We must first provide a formal definition of what is meant by "effective operator".

Definition III.1. *A time dependent operator O^{eff} is known as an effective operator if it includes the time evolution and measurement settings of an open quantum system, such that expectation values of measurements corresponding to those settings are described by*

$$E = Tr[O^{eff}(\alpha, \phi, t)\rho]. \tag{128}$$

Following this definition, we may now obtain the matrix form of the effective operator corresponding to the neutral kaon system. The expectation value, in terms of the short and long-lived elements of the density operator, is

$$E = Tr(O^{eff}\rho)$$

$$= 2P(Y : k_n, t_n) - 1$$

$$= 2(\rho_{SS}cos^2\frac{\alpha_n}{2}e^{-\Gamma_S t_n} + \rho_{LL}sin^2\frac{\alpha_n}{2}e^{-\Gamma_L t_n} \tag{129}$$

$$+ \rho_{SL}cos\frac{\alpha_n}{2}sin\frac{\alpha_n}{2}e^{i(\phi_n-t_n)}e^{-\Gamma t_n}$$

$$+ \rho_{LS}cos\frac{\alpha_n}{2}sin\frac{\alpha_n}{2}e^{-(i\phi_n-t_n)}e^{\Gamma t_n}) - 1.$$

Considering an initial pure state

$$\rho = |\phi\rangle\langle\phi|,$$

with $|\phi\rangle = \frac{1}{\sqrt{2}}(|K_S\rangle + |K_L\rangle)$, we may rewrite the above expectation value as:

$$Tr(O^{eff}|\phi\rangle\langle\phi|) = \langle\phi|O^{eff}|\phi\rangle = \frac{1}{2}(\langle K_S| + \langle K_L|)O^{eff}(|K_S\rangle + |K_L\rangle) \tag{130}$$

Identifying the elements of Eq.(130) with the ones from Eq.(129), one obtains the desired matrix form of the effective operator, in the lifetime eigenbasis

$$O^{eff}(\alpha_n, \phi_n, t_n) = \begin{pmatrix} cos^2\frac{\alpha_n}{2}e^{-\Gamma_S t_n} - 1 & cos\frac{\alpha_n}{2}sin\frac{\alpha_n}{2}e^{i(\phi_n-t_n)}e^{-\Gamma t_n} \\ cos\frac{\alpha_n}{2}sin\frac{\alpha_n}{2}e^{-i(\phi_n-t_n)}e^{-\Gamma t_n} & sin^2\frac{\alpha_n}{2}e^{-\Gamma_L t_n} - 1 \end{pmatrix} \tag{131}$$

A few remarks are in order: first, from the matrix form of this operator, we see that for large times, when the probability that the particles have decayed is very high, the effective operator tends to minus identity. This is a reasonable expectation, since, as the particles decay, the overall amount of detection events decreases; second, using the definition Eq.(128), it is easy to observe that, for a number of m particles, the expectation value can be generalized simpy as

$$E = Tr[O_1^{eff} \otimes O_2^{eff} \otimes ... \otimes O_m^{eff}\rho_m], \tag{132}$$

where O_i^{eff} acts on the i-th subsystem, with its corresponding measurement settings and measurement times, and ρ_m represents the m-particle initial state.

It is also useful to decompose the effective operator in the Pauli basis. Because it corresponds to an open system,

$$O^{eff} = -n_0 \mathbb{1} + \vec{n} \cdot \vec{\sigma}, \tag{133}$$

where the explicit dependence on α, θ and t has been omitted for brevity. The component n_0 increases as the system decays, playing the role of "white" noise. Determining the individual elements is done by projecting the effective operator onto each of the corresponding Pauli matrices. For the first element, we have

$$
\begin{aligned}
n_1 &= Tr(O^{eff}\sigma_1) \\
&= Tr\left[O^{eff} \begin{pmatrix} 0 & 1 \\ 1 & 0 \end{pmatrix} \right] \\
&= Tr \begin{pmatrix} \cos\frac{\alpha_n}{2}\sin\frac{\alpha_n}{2}e^{i(-\phi_n - t_n)}e^{-\Gamma t_n} & \cos^2\frac{\alpha_n}{2}e^{-\Gamma_s t_n} - 1 \\ \sin^2\frac{\alpha_n}{2}e^{-\Gamma_L t_n} - 1 & \cos\frac{\alpha_n}{2}\sin\frac{\alpha_n}{2}e^{-i(-\phi_n - t_n)}e^{-\Gamma t_n} \end{pmatrix} \\
&= \cos\frac{\alpha_n}{2}\sin\frac{\alpha_n}{2}e^{i(-\phi_n - t_n)}e^{-\Gamma t_n} + \cos\frac{\alpha_n}{2}\sin\frac{\alpha_n}{2}e^{-i(-\phi_n - t_n)}e^{-\Gamma t_n} \\
&= \cos\frac{\alpha_n}{2}\sin\frac{\alpha_n}{2}e^{-\Gamma t_n} \cdot 2\cos(\phi_n - t_n)
\end{aligned}
\tag{134}
$$

In a similar way, by projecting O^{eff} onto the other two Pauli matrices, one obtains

$$
\begin{aligned}
n_2 &= \sin(\phi_n + t_n)\sin(\alpha_n)e^{-\Gamma t_n} \\
n_3 &= \cos\alpha_n \cosh(\Delta\Gamma t_n)e^{-\Gamma t_n} + \sinh(\Delta\Gamma t_n)e^{-\Gamma t_n},
\end{aligned}
\tag{135}
$$

with $\Delta\Gamma = \Gamma_S - \Gamma_L$. In order for the time evolution described by O^{eff} to be trace-preserving, we must impose the condition that

$$n_0 = 1 - |\vec{n}|. \tag{136}$$

With all the above results, the vector $\vec{n}$ has the final form

$$\vec{n} = e^{-\Gamma t_n} \begin{pmatrix} \cos(t_n - \phi_n)\sin(\alpha_n) \\ \sin(t_n - \phi_n)\sin(\alpha_n) \\ \cos\alpha_n \cosh(\Delta\Gamma t_n) + \sinh(\Delta\Gamma t_n) \end{pmatrix}. \tag{137}$$

d. *Eigenvalues and Eigenvectors of O^{eff}*

Using the matrix form of O^{eff} from Eq.(131), we can proceed to solving the eigenvalue equation

$$O^{eff} |\chi_i\rangle = \lambda_i |\chi_i\rangle \tag{138}$$

Solving this equation, we obtain the following values for λ and $|\chi\rangle$:

$$\lambda_1 = cos^2\frac{\alpha_n}{2}e^{-\Gamma_S t_n} + sin^2\frac{\alpha_n}{2}e^{-\Gamma_L t_n} - 1$$
$$\lambda_2 = 1 \tag{139}$$

corresponding to the eigenvectors:

$$|\chi_1\rangle = \frac{1}{\sqrt{N}}(cos\frac{\alpha_n}{2}e^{-\frac{\Gamma_S}{2}t_n}|K_S\rangle + e^{i(t_n-\phi_n)}e^{-\frac{\Gamma_L}{2}t_n}sin\frac{\alpha_n}{2}|K_L\rangle)$$
$$|\chi_2\rangle = \frac{1}{\sqrt{N}}(sin\frac{\alpha_n}{2}e^{-\frac{\Gamma_L}{2}t_n}|K_S\rangle + e^{i(t_n-\phi_n)}e^{-\frac{\Gamma_S}{2}t_n}cos\frac{\alpha_n}{2}|K_L\rangle) \tag{140}$$

where the lifetime eigenstates $|K_S\rangle$ and $|K_L\rangle$ have been chosen to represent the computational basis vectors $|0\rangle$ and $|1\rangle$.

The eigenvector $|\chi_1\rangle$ can be seen as the quasi-spin $|k_n\rangle$, evolving according to the system's Hamiltonian and being normalized to the surviving kaons [18].

e. *Introducing CP-violation*

The effective operator we have so far does not provide a complete description of the neutral kaon system, due to the fact that we have neglected the phenomenon of CP-violation. In

45

what follows, the elements of the effective operator matrix, in the lifetime eigenbasis, will be included, where we take violation of CP-symmetry into account. Afterwards, the two Bell-type inequalities previously mentioned [See Eq.(9) and Eq.(13)] will be written in terms of the effective operator and results will be presented.

With the introduction of the phenomenon of CP violation, the eigenstates of the system's Hamiltonian, namely $|K_S\rangle$ and $|K_L\rangle$ are no longer the same as the eigenstates of the CP operator. To account for the slight non-orthogonality of the lifetime states, the ϵ parameter is added, in the form of p and q, as in Eq.(107). A useful quantity, in terms of p and q is

$$\delta = \frac{|p|^2 - |q|^2}{|p|^2 + |q|^2} \tag{141}$$

which will be used later, in order to simplify notation. The matrix elements of the initial state, in terms of the strangeness eigenstates, are thus

$$\rho_{SS} = |K_S\rangle\langle K_S| = \frac{1}{|N|^2}(p^2 |K^0\rangle\langle K^0| - pq |K^0\rangle\langle \bar{K}^0| - pq |\bar{K}^0\rangle\langle K^0| + q^2 |\bar{K}^0\rangle\langle \bar{K}^0|),$$

$$\rho_{SL} = |K_S\rangle\langle K_L| = \frac{1}{|N|^2}(p^2 |K^0\rangle\langle K^0| + pq |K^0\rangle\langle \bar{K}^0| - pq |\bar{K}^0\rangle\langle K^0| - q^2 |\bar{K}^0\rangle\langle \bar{K}^0|),$$

$$\rho_{LS} = |K_L\rangle\langle K_S| = \frac{1}{|N|^2}(p^2 |K^0\rangle\langle K^0| - pq |K^0\rangle\langle \bar{K}^0| + pq |\bar{K}^0\rangle\langle K^0| - q^2 |\bar{K}^0\rangle\langle \bar{K}^0|),$$

$$\rho_{LL} = |K_L\rangle\langle K_L| = \frac{1}{|N|^2}(p^2 |K^0\rangle\langle K^0| + pq |K^0\rangle\langle \bar{K}^0| + pq |\bar{K}^0\rangle\langle K^0| + q^2 |\bar{K}^0\rangle\langle \bar{K}^0|).$$

Starting from these expressions, we begin calculating the elements of

$$O^{eff} = \begin{pmatrix} \langle K_S| O^{eff} |K_S\rangle & \langle K_S| O^{eff} |K_L\rangle \\ \langle K_L| O^{eff} |K_S\rangle & \langle K_L| O^{eff} |K_L\rangle \end{pmatrix}. \tag{142}$$

In order to avoid cumbersome calculations, the first term will be derived in detail while the other three will be written down in their final form, since they are obtained in an analogous manner.

Referring to Eq.(129) and (131), one can write the first matrix element as

$$\langle K_S | O^{eff} | K_S \rangle = 2(\langle K_S | \rho_{SS} | K_S \rangle \cos^2 \frac{\alpha_n}{2} e^{-\Gamma_S t_n}$$

$$+ \langle K_S | \rho_{LL} | K_S \rangle \sin^2 \frac{\alpha_n}{2} e^{-\Gamma_L t_n}$$

$$+ \langle K_S | \rho_{SL} | K_S \rangle \cos \frac{\alpha_n}{2} \sin \frac{\alpha_n}{2} e^{i(\phi_n - t_n)} e^{-\Gamma t_n}$$

$$+ \langle K_S | \rho_{LS} | K_S \rangle \cos \frac{\alpha_n}{2} \sin \frac{\alpha_n}{2} e^{-i(\phi_n - t_n)} e^{-\Gamma t_n}) - 1. \qquad (143)$$

Each of the elements above can be further written as [Eq.(107)]

$$\langle K_S | \rho_{SS} | K_S \rangle = \frac{1}{|N|^2} (\langle K^0 | p - \langle \bar{K}^0 | q) \rho_{SS} (p | K^0 \rangle - q | \bar{K}^0 \rangle)$$

$$= \frac{1}{|N|^4} (p^4 + 2p^2 q^2 + q^4)$$

$$= \frac{1}{|N|^2},$$

and, the other three can be deduced in the same manner

$$\langle K_S | \rho_{LL} | K_S \rangle = \langle K_S | \rho_{LS} | K_S \rangle = \langle K_S | \rho_{SL} | K_S \rangle = \frac{\delta^2}{|N|^2}$$

and with these, one finds the first matrix element of the effective operator as

$$\langle K_S | O^{eff} | K_S \rangle = \frac{2}{|N|^2} \cos^2 \frac{\alpha_n}{2} e^{-\Gamma_S t_n}$$

$$+ \frac{2\delta^2}{|N|^2} \sin^2 \frac{\alpha_n}{2} e^{-\Gamma_L t_n}$$

$$+ \frac{2\delta}{|N|^2} \cos \frac{\alpha_n}{2} \sin \frac{\alpha_n}{2} e^{i(\phi_n - t_n)} e^{-\Gamma t_n} \qquad (144)$$

$$+ \frac{2\delta}{|N|^2} \cos \frac{\alpha_n}{2} \sin \frac{\alpha_n}{2} e^{-i(\phi_n - t_n)} e^{-\Gamma t_n}) - 1.$$

Similarly, the other three matrix elements of O^{eff} can be found as

$$\langle K_S | \tilde{O}^{eff} | K_L \rangle = \frac{2\delta}{|N|^2} \cos^2 \frac{\alpha_n}{2} e^{-\Gamma_S t_n}$$

$$+ \frac{2\delta}{|N|^2} \sin^2 \frac{\alpha_n}{2} e^{-\Gamma_L t_n}$$

$$+ \frac{2}{|N|^2} \cos \frac{\alpha_n}{2} \sin \frac{\alpha_n}{2} e^{i(\phi_n - t_n)} e^{-\Gamma t_n} \qquad (145)$$

$$+ \frac{2\delta^2}{|N|^2} \cos \frac{\alpha_n}{2} \sin \frac{\alpha_n}{2} e^{-i(\phi_n - t_n)} e^{-\Gamma t_n}) - \delta,$$

47

$$\langle K_L | O^{eff} | K_S \rangle = (\langle K_S | \tilde{O}^{eff} | K_L \rangle)^* = \frac{2\delta}{|N|^2} \cos^2 \frac{\alpha_n}{2} e^{-\Gamma_S t_n}$$
$$+ \frac{2\delta}{|N|^2} \sin^2 \frac{\alpha_n}{2} e^{-\Gamma_L t_n}$$
$$+ \frac{2}{|N|^2} \cos \frac{\alpha_n}{2} \sin \frac{\alpha_n}{2} e^{-i(\phi_n - t_n)} e^{-\Gamma t_n}$$
$$+ \frac{2\delta^2}{|N|^2} \cos \frac{\alpha_n}{2} \sin \frac{\alpha_n}{2} e^{i(\phi_n - t_n)} e^{-\Gamma t_n}) - \delta, \tag{146}$$

and finally, the last element

$$\langle K_L | O^{eff} | K_L \rangle = 2(\langle K_L | \rho_{SS} | K_L \rangle \cos^2 \frac{\alpha_n}{2} e^{-\Gamma_S t_n}$$
$$+ \langle K_L | \rho_{LL} | K_L \rangle \sin^2 \frac{\alpha_n}{2} e^{-\Gamma_L t_n}$$
$$+ \langle K_L | \rho_{SL} | K_L \rangle \cos \frac{\alpha_n}{2} \sin \frac{\alpha_n}{2} e^{i(\phi_n - t_n)} e^{-\Gamma t_n}$$
$$+ \langle K_L | \rho_{LS} | K_L \rangle \cos \frac{\alpha_n}{2} \sin \frac{\alpha_n}{2} e^{-i(\phi_n - t_n)} e^{-\Gamma t_n}) - 1. \tag{147}$$

f. Bell Inequalities and Results

Having a detailed description of our formalism, it's now time to look at its predictions. In Section I, we introduced two Bell-type Inequalities: the CHSH inequality in Eq.(9) and the SCG inequality, in Eq.(13), and we justified the latter by the fact that there exist states which violate it and do not violate the original CHSH. In the results section, we will also see that the optimal violation of the SCG inequality is significantly larger, and, when we will discuss the general formalism and vary ϵ, an intriguing result will appear, namely a much stronger robustness to a variation of this parameter in the SCG as opposed to the CHSH inequality. First, to apply our formalism, the two inequalities must be written in their "witness" form, namely

$$CHSH^{eff} = O_n^{eff} \otimes (O_m^{eff} - O_{m'}^{eff}) + O_{n'}^{eff} \otimes (O_m^{eff} + O_{m'}^{eff}), \tag{148}$$

and

$$
\begin{aligned}
SCG^{eff} =\, &O^{eff}(m) \otimes (\mathbb{1} + O^{eff}(n) + O^{eff}(n') + O^{eff}(p)) \\
&+ O^{eff}(m') \otimes (\mathbb{1} + O^{eff}(n) + O^{eff}(n') - O^{eff}(p)) \\
&+ O^{eff}(k) \otimes (O^{eff}(n) - O^{eff}(n')) \\
&+ \mathbb{1} \otimes (O^{eff}(n) - O^{eff}(n')).
\end{aligned}
\tag{149}
$$

The parameters m, n, k, m', n', p', represent the measurement settings of the two experimenters, Alice and Bob. In our case, they represent (fixed) measurement angles and different times, for example $m = \{\alpha_m, \phi_m, t_m\}$. The constraints that must be obeyed by all local-realistic hidden variable theories are

$$
|Tr[CHSH^{eff}\rho_0]| \leq 2,
\tag{150}
$$

and

$$
Tr[SCG^{eff}\rho_0] \geq -4,
\tag{151}
$$

respectively. ρ_0 is just a time-independent two-particle initial state. One important feature of the effective formalism is that one does not need to perform optimizations over all initial states, the optimal violations are found within the eigenvalues of the effective operators, so we will ignore ρ_0 altogether.

The experimental set-up of a Bell-test is rather standard: a pair of particles produced at a source propagate in opposite directions. They are detected by two experimenters, by tradition named Alice and Bob. There are two possible ways to test any given Bell-type inequality in this situation:

- Fix the measurement times and measure for different quasi-spins.

- Fix the quasi-spins and measure at different times.

Because of the scarcity of directions when it comes to choosing a quasi-spin, the former option does not provide interesting information, other than what would be, much easier, obtained with non-decaying systems like photons. However, the decay and strangeness oscillation make the latter much more appealing. In short, both Alice and Bob agree upon
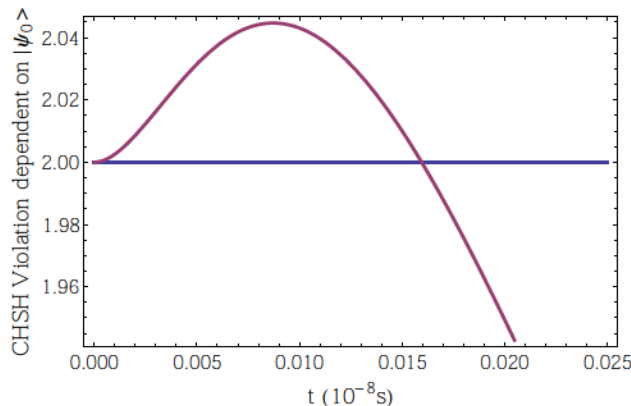
FIG. 10: Violation of the CHSH inequality starting with fixed initial state.

a single measurement direction, say $\bar{K}^0$ and each measures his or her particle at a different time.

In Fig. 10, we reproduce a plot of Eq.(150), considering a fixed initial state $\rho_0 = |\psi\rangle\langle\psi|$, where $|\psi\rangle$ is a Bell-state in the strangeness eigenbasis. While a violation is observed, it's important to note that this is not the maximum one can obtain within this system.

In order to find a maximal violation, one must consider the eigenvalues of the effective operator, thus in Fig. 11 we present two such eigenvalue plots, corresponding to the CHSH and SCG inequalities. The measurement settings for the CHSH in subfigure (a) are $A(0,\tau)$ and $B(\tau,0)$, meaning that Alice performed two measurements, one at $t_{A1} = 0$ and the other at $t_{A2} = \tau$ and Bob measured at $t_{B1} = \tau$ and $t_{B2} = 0$, in every instance the quasi-spin direction remained fixed ($|\bar{K}^0\rangle$) where τ is a plot parameter.

The numerical values obtained, for the neutral kaon CP-violation constant $\epsilon \approx 10^{-3}$ are $V_{CHSH} \approx 0.11$ and $V_{SCG} \approx 1.58$.

In the following, we will present a generalization of this effective formalism, that can be applied to any multilevel decaying system, which also retains an oscillating behaviour similar to strangeness oscillations. We then go on to provide results on a two-level kaon-like model, where we can treat ϵ as a variable, and illustrate the robustness to its variation of both inequalities. In the end, we will provide two detailed methods of implementing such a model with trapped ions.

The plot for the eigenvalues of the CHSH inequality in Fig. 11-(a) reproduces the results from Ref. [18]. Violations of this inequality can be found for other symmetric measurement
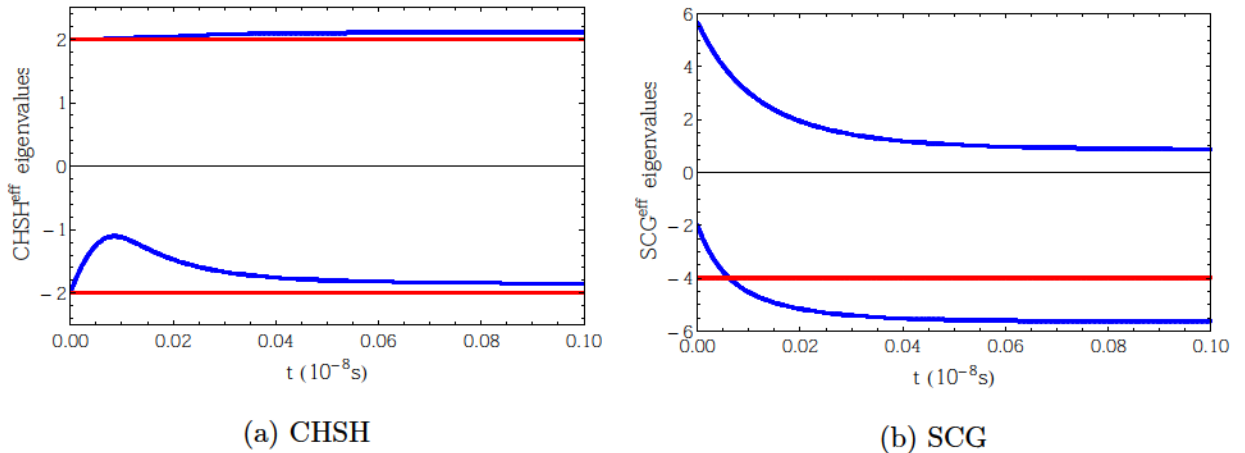
50

(a) CHSH

(b) SCG

FIG. 11: Minimal and maximal eigenvalues of $CHSH^{eff}$ and SCG^{eff} with the corresponding limits.

settings as well, for example $A(\tau, 0)$ and $B(0, \tau)$. Detailed plots, for various values of ϵ are presented in Appendix B.

2. General Effective Formalism

In this section we describe our generalization of the effective operator formalism. Later, we will see how it can be applied to other systems beyond neutral kaons. This generalization is based on the Bloch equation formalism [6]. We start by treating a closed three-level system at zero temperature, with population decay from the upper two levels to a ground level (see Fig. 12)

The long and short-lived states $|K_S\rangle$ and $|K_L\rangle$ would correspond to $|2\rangle$ and $|1\rangle$, respectively. The $|0\rangle$ level plays the role of a general "decayed" level.

The time evolution of a single particle is given by the Lindblad equation

$$\dot{\rho}(t) = -i[H, \rho(t)] - \sum_i \gamma_i (\frac{1}{2}\{\Lambda_i^\dagger \Lambda_i, \rho(t)\} - \Lambda_i \rho(t)\Lambda_i^\dagger), \tag{152}$$

with Λ_i being jump operators between different levels. Here, H is the mass term M from Eq.(105), a notation we will maintain throughout the rest of the section. For our case, these

The derivations and results presented in this and the following section have been published as part of [38]

51
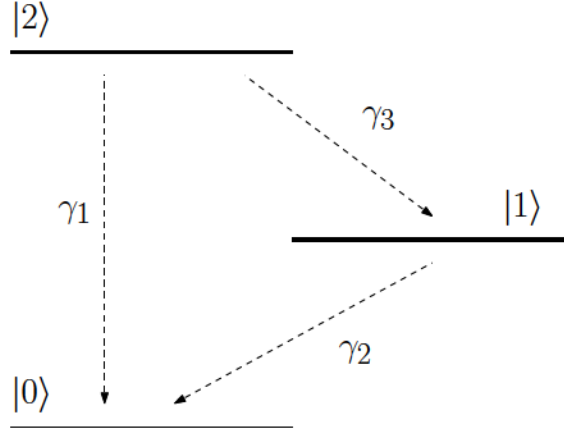
FIG. 12: A general three-level system at zero temperature with different decay processes. See the text for further details.

are given by

$$\Lambda_{20} = |0\rangle \langle 2| ,$$
$$\Lambda_{21} = |1\rangle \langle 2| ,$$
$$\Lambda_{10} = |0\rangle \langle 1| .$$

(153)

Taking into account only the unitary part of the time evolution

$$\dot{\rho}(t) = -i[H, \rho(t)],$$

(154)

and denoting the density operator in column vector form as

$$\vec{\rho} = (\rho_{1,1}, ..., \rho_{1,N}, \rho_{2,1}, ..., \rho_{2,N}, ..., \rho_{N,N})$$

(155)

the unitary part becomes

$$-i[H, \rho] = -i(H \otimes \mathbb{1} - \mathbb{1} \otimes H^T)\vec{\rho}.$$

(156)

As for the non-unitary part of the time evolution, we simplify the notation by writing it as

$$\dot{\rho} = \frac{-\gamma}{2}(\Lambda_+ \Lambda_- \rho + \rho \Lambda_+ \Lambda_- - 2\Lambda_- \rho \Lambda_+),$$

(157)

where Λ_+ stands for $\Lambda^\dagger$ and Λ_- stands for Λ.

Using the transformation from Eq. (156), we have

$$\Lambda_+ \Lambda_- \cdot \rho = (\Lambda_+ \Lambda_- \otimes \mathbb{1})\vec{\rho},$$
$$\rho \cdot \Lambda_+ \Lambda_- = (\mathbb{1} \otimes (\Lambda_+ \Lambda_-)^T)\vec{\rho},$$
$$\Lambda_- \rho \Lambda_+ = \Lambda_- \cdot (\rho \Lambda_+) = (\Lambda_- \otimes \mathbb{1}) \cdot (\mathbb{1} \otimes \Lambda_+^T)\vec{\rho}.$$
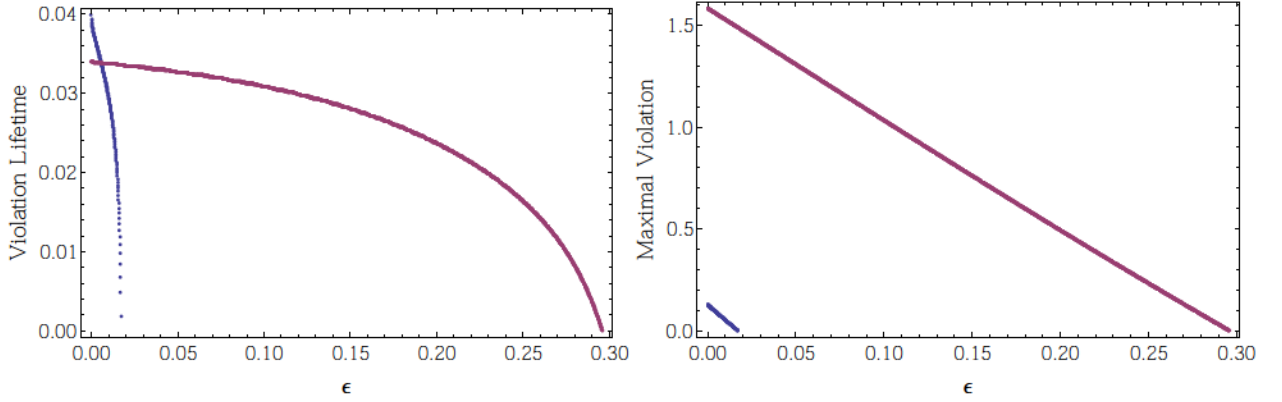
(158)

FIG. 13: Comparison of the ϵ-dependence of the violation lifetime and maximal violation for the CHSH and SCG inequalities.

The Lindblad equation can now be written in operator form

$$\vec{\dot{\rho}} = A\vec{\rho}, \tag{159}$$

with the time evolution operator given by the above results

$$
\begin{aligned}
A =& [-i(H \otimes \mathbb{1} - \mathbb{1} \otimes H^T) \\
& - \frac{\gamma}{2}(\Lambda_+\Lambda_- \otimes \mathbb{1} + \mathbb{1} \otimes \Lambda_+\Lambda_- - 2\Lambda_- \otimes \Lambda_-)].
\end{aligned} \tag{160}
$$

Note that, while for the specific way in which we have defined the Λ operator, the relation $\Lambda_+^T = \Lambda_-$ holds, this is not true in general. With this, the time evolution equation of the decaying system is simply

$$\vec{\rho}(t) = e^{At}\vec{\rho}(0). \tag{161}$$

Worth mentioning is that this formulation of the time evolution also makes a numerical approach towards solving the problem possible.

The final step is to construct the general effective operator. From Eq. (128) - (129) it follows that

$$E = Tr[2\left|k_n\right\rangle \left\langle k_n\right| \rho(t) - \rho(0)], \tag{162}$$

where we used the fact that $Tr[\rho(0)] = 1$. In order to apply the time evolution, we will write everything in vector notation and then go back to the original matrix notation, to recover

53

the final form of the effective operator. Denoting the matrix $|k_n\rangle \langle k_n|$ as K, we have

$$
\begin{aligned}
E &= Tr[2(K \otimes \mathbb{1})\vec{\rho}(t) - \vec{\rho}(0)] \\
&= Tr[2(K \otimes \mathbb{1})e^{At}\vec{\rho}(0) - \vec{\rho}(0)],
\end{aligned}
\tag{163}
$$

see Eq. (161). In vector notation, one should retain the indices from the matrix notation ($\rho_{i,j}$), in order for the trace to make sense, thus, in the above equation, the trace should be understood as

$$
Tr[\vec{\rho}(t)] = \sum_i \vec{\rho}_{ii}(t).
\tag{164}
$$

Finally, we apply the exponential to $\vec{K}$ and revert to the original matrix notation, where we replace $\vec{K}e^{At}$ with $K(t)$

$$
\begin{aligned}
E &= Tr[(2K(t) - \mathbb{1})\rho(0)] \\
&= Tr[O^{\text{eff}}\rho(0)],
\end{aligned}
\tag{165}
$$

from which one can simply identify the general effective operator as

$$
O^{\text{eff}}(k_n, t_n) = 2K(k_n, t_n) - \mathbb{1}.
\tag{166}
$$

Here, the dependence of K on the time t_n and measurement direction k_n has been explicitly highlighted.

The above effective operator represents measurements performed on a single particle, and the possible settings are given by the measurement "angles" of the quasi-spin and the various times. Now, as previously mentioned, one can test correlations between larger numbers of particles, by taking the tensor products of the corresponding effective operators.

3. Experimental Implementation

a. General Considerations

Before looking at two examples of kaon-like behaviour in trapped Yb ions we summarize the general requirements for simulating kaon-like behaviour with ions.
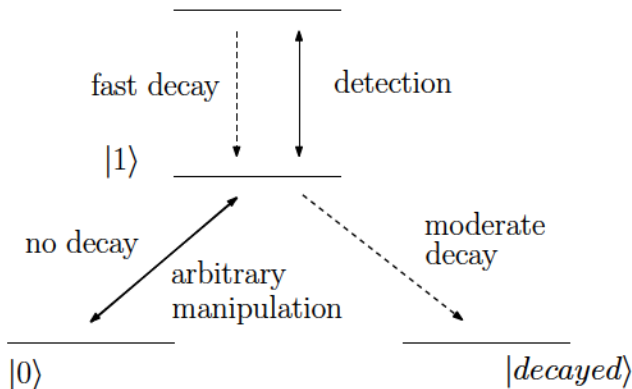
FIG. 14: Basic scheme needed to implement kaon-like behaviour

As shown in Fig. 14, there must be two levels which we identify as $|1\rangle = |K_1^0\rangle$ and $|0\rangle = |K_2^0\rangle$ and consecutively $|K_0\rangle = |+\rangle$ and $|\bar{K}_0\rangle = |-\rangle$ with $|\pm\rangle = (|0\rangle \pm |1\rangle)/\sqrt{2}$. There should be no decay between these two levels (as there is no decay between $|K_1^0\rangle \approx |K_S\rangle$ and $|K_2^0\rangle \approx |K_L\rangle$). Beside a two-qubit gate to create entanglement also arbitrary singe-qubit rotations (for example by using an RF-field) are needed for preparation, inducing kaon oscillation and choosing arbitrary measurement directions.

Without CP violation, the oscillation between $|K^0\rangle$ and $|\bar{K}^0\rangle$ corresponds to an oscillation around the $z-$axis given by $U(t) = \exp(-i\delta t \sigma_z)$ with the Pauli matrix σ_z. The rotation frequency δ is given by the detuning $\delta = \omega_K - \omega_L$ between the level splitting ω_K and the reference laser ω_L determining the rotating reference frame.

The CP violation ε leads to several effects. For example $|K^0(t)\rangle$ is decaying faster than $|\bar{K}^0(t)\rangle$ and the decay rate for both states start to oscillate. Furthermore their expectation values $\langle \sigma_z(t) \rangle$ undergo small oscillations and we find $\langle \sigma_z(t) \rangle_{K^0} \geq \langle \sigma_z(t) \rangle_{\bar{K}^0}$ for all times. This behaviour can be simulated by slightly tilting the rotation axis. The connection between the CP violation and the tilting is given by

$$\frac{\delta}{\sqrt{\delta^2 + \Omega^2}} = \frac{1 - \varepsilon}{1 + \varepsilon} \tag{167}$$

with the Rabi frequency Ω determining the strength of the laser or microwave.

Two additional levels are needed, one for fluorescence detection (from which a fast decay must exist to one of the qubit states) and another, representing the state of decay products, with a moderate decay rate Γ_S from one of the two qubit states.

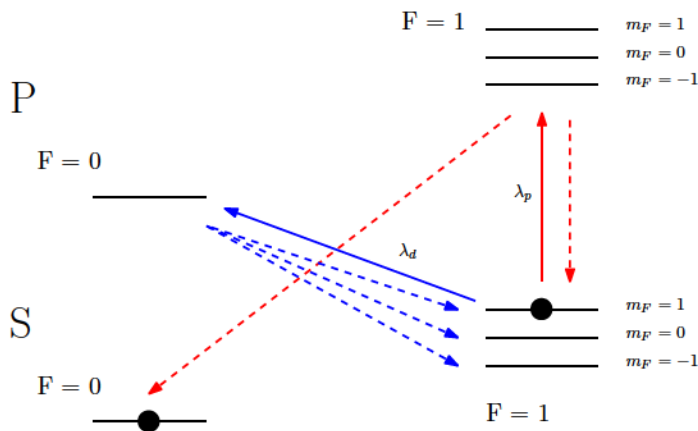In general, arbitrary values for the oscillation frequency ω, the decay rate Γ_S and the CP-

FIG. 15: An implementation of the effective formalism using $^{171}Yb^+$. The qubit is defined between the two levels marked with thick dots.

violation ε can be choosen for our ion system. However, the behaviour of the here described ion system mimics kaon-like behaviour only for small values of the CP violation, that is $\varepsilon \ll \omega/\Gamma_S$. This becomes apparent if we look at Eq. (97) which leads to unphysical behaviour for large ε.

In the following, we propose two examples of experimentally testing the predictions of our effective formalism, using trapped Ytterbium isotopes.

b. *Example 1*

The first proposal is based on the level structure of $^{171}Yb^+$ sketched in Fig. 15. The qubit is defined as $|0\rangle = |S, F = 0\rangle$ and $|1\rangle = |S, F = 1, m_F = 1\rangle$ and the decayed state is represented by $|S, F = 1, m_F = 0\rangle$ and $|S, F = 1, m_F = -1\rangle$. $|0\rangle$ and $|1\rangle$ are both long-lived states. However, decay can be generated by weak driving of the $|S, F = 1, m_F = 1\rangle \leftrightarrow |P, F = 0\rangle$ transition with σ^- polarized light. From $|P, F = 0\rangle$ the state decays fast to all $|S, F = 1, m_F\rangle$ states. It is important to note here that the strength of the decay is thus tunable, by tuning the strength / duration of the transitions.

This decay behaviour is slightly different from kaons, because $|0\rangle$ does not decay and there is a non-zero probability of $|1\rangle$ "decaying" to itself, which leads to dephasing. More clearly,
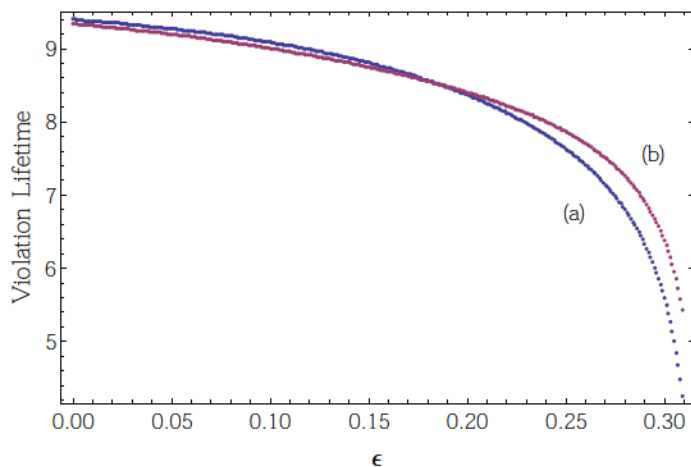
56

FIG. 16: The effect of dephasing on the violation lifetimes (units of 10ns) for the SCG inequality, in terms of ϵ. Here we plot both the case of (a) only decay with strength γ_S and (b) splitting γ_S into 2/3 decay and 1/3 dephasing.

while for neutral kaons one could express the decay process as

$$\Gamma = \gamma_S \left|decayed\right\rangle \left\langle 1\right| + \gamma_L \left|decayed\right\rangle \left\langle 0\right|, \tag{168}$$

where, for clarity of notation, the short-lived kaon state has been identified with $\left|1\right\rangle$ and long-lived kaon state with $\left|0\right\rangle$; the case for the example 1 is described by

$$\Gamma' = \gamma_S \left(\frac{2}{3} \left|decayed\right\rangle \left\langle 1\right| + \frac{1}{3} \left|1\right\rangle \left\langle 1\right| \right), \tag{169}$$

where there is always a chance of decay to the initial level (dephasing). In Fig. 16 we plot the violation lifetimes in terms of the CP-violation parameter with and without splitting γ_S into 2/3 decay and 1/3 dephasing.

The essence of the effective formalism is that it does not distinguish between a non-detection event and one of the two possible states (decayed or $\left|K^0\right\rangle$, when measuring $\left|\bar{K}^0\right\rangle$, in the kaon case). This could be translated into

$$\underbrace{P_{\left|\bar{K}^0\right\rangle}}_{P(Y)} + \underbrace{P_{\left|K^0\right\rangle} + P_{decayed}}_{P(N)} = 1. \tag{170}$$

This provides the option of performing the opposite measurement (corresponding to $P(N)$ above). For this , we perform a population inversion between the $\left|S, F = 1\right\rangle$ sublevels and the $\left|S, F = 0\right\rangle$ level. Then, a typical fluorescence measurement can be performed on the S level.

57

There is also a second option to perform the population inversion and that is a population shelving from the two sublevels, representing the decayed state, to some other atomic level.

Another necessary step to simulate kaon is to generate entanglement between two ions. This is achieved in our example by using MAGIC (Magnetic Gradient-Induced Coupling) [28, 34].

State detection of the ion is achieved by a single qubit rotation to choose the measurement direction and consecutively driving the $|S, F = 1\rangle \leftrightarrow |P, F = 0\rangle$ transition with unpolarized light and detecting the scattered photons.Unfortunately, this state dependent fluorescence measurement is only able to distinguish between the states $|S, F = 0\rangle$ and $|S, F = 1\rangle$, but cannot resolve the sublevels $|m_F = 0, 0/ \pm 1\rangle$. Therefore, each probability measured in such a way will correspond to the sum of the probability $P(|k_n\rangle)$ to be in the state $|k_n\rangle$ plus the probability that the ion/kaon has already decayed. Therefore, instead of measuring $P(|\bar{K}_0\rangle)$ we rotate $|K_0\rangle = |+\rangle$ onto the state $|1\rangle$ and perform in this way an inverse measurement and determine the propbability $P = 1 - P(|\bar{K}_0\rangle)$. That is, instead of asking "What is the probability corresponding to the state $|\bar{K}^0\rangle$, we may equivalently ask "What is the probability for not obtaining $|\bar{K}_0\rangle$?".

c. Example 2

A second way to implement the formalism is to use $^{172}Yb^+$ ions. In this case, the qubit is defined between the $|D_{3/2}, m_j = -3/2\rangle$ and $|D_{3/2}, m_j = -1/2\rangle$ levels (Fig. 17).

The implementation is done by running a pump laser between the S and P states, this leads to a population transfer to all four $D_{3/2}$ sublevels, due to decay. Then a combination of π and σ_- polarized lasers move the populations of the upper three D sublevels to the $|[3/2, 1/2]\rangle$ states, and ultimately to the $|D_{3/2}, m_j = -3/2\rangle$ sublevel.

Coherent driving of the $|D_{3/2}, m_j = -3/2\rangle \leftrightarrow |D_{3/2}, m_j = -1/2\rangle$ transition causes a problem, because the level splitting of all $|D_{3/2}\rangle$ states are equal. To isolate this transition, an AC Stark shift is induced, to increase the distance between the qubit levels and the sublevels $m_j = 1/2$ and $m_j = 3/2$.

The decay is modelled by a weak pulse driving the transitions $|D_{3/2}, m_j = -1/2\rangle \leftrightarrow |P_{1/2}\rangle$.
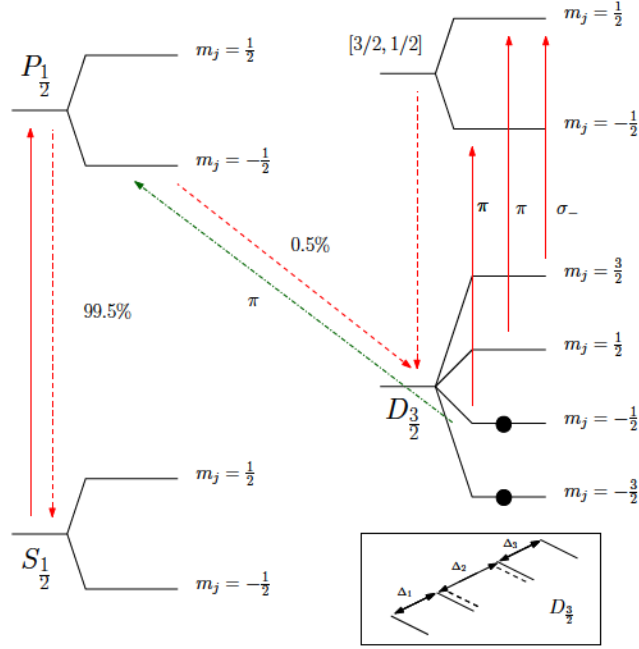
FIG. 17: An implementation of the effective formalism using ^{172}Yb$^+$. The qubit is defined between the two levels marked with thick dots. The effect of the AC Stark shift is also shown in the lower box.

Finally, we transfer again the state $|K^0\rangle$ onto $|P\rangle$ before performing a state dependent fluorescence measurement by driving the $|S\rangle \leftrightarrow |P\rangle$ transition. This measurement is again an inverse measurement similar to the first example, essentially measuring the probability $1 - P(\bar{K}^0)$ (using kaon notation).

In both examples, two ions can be entangled with the help of MAGIC [28, 34] to generate a bipartite system with similar properties as pairs of neutral kaons.

Two remarks need to be made here. First, the time evolution of "decay" and "oscillation" commute only for $\varepsilon = 0$. In this case, we are able to switch on the lasers/microwaves causing the decay and the oscillation one after the other. However, for $\varepsilon \neq 0$ our way to model interfere with the oscillation. Therefore, we have to use the Trotter theorem and approximated the time evolution by switching between oscillation and decay in short time intervals. This is a standard method in digital quantum simulations and the approximation can be made arbitrarily good by shorting e.g. the time intervals (see e.g. [30]).

Second, as explained above, there are different decay channels between kaons and the chosen ion examples [compare Eq.(168) and Eq.(169)]. This does not significantly modify

59

the nature results for small CP violations ϵ as depicted in Fig.16.

4. Summary

The reasons for an effective operator formulation of an open system are better control of state normalization and easier generalization to multipartite systems. The existing formalism [18] was designed around the characteristics of neutral kaons and provided a method for entanglement detection. Our task was to generalize this formalism to arbitrary open quantum systems and suggest an application to the case of trapped Ytterbium ions. The chosen level schemes and manipulation techniques allowed the simulation of kaon behaviour and thus we could reproduce the results of the initial formalism. The effective operator also allows reducing time evolution to a matrix exponentiation operation, thus making numerical implementations easier.

One could further generalize the formalism to include multilevel systems and decay schemes, for example decay between two levels that are not considered part of the environment, or the introduction of artificial oscillations and state non-orthogonality, which could be useful in studying noise and imperfect state preparation upon the entanglement initially present in the system.

IV.   Introduction to Semidefinite Programming

In the following section we describe a method for obtaining genuinely multipartite entangled states, with separable two-body marginals. The method uses two semidefinite programs for optimizing the violation of a witness, by applying one program on the witness and the second on the state. Before that, however, we need to consider this optimization procedure in some detail, which is the purpose of this section.

A.   Linear Programming (LP)

Prior to discussing semidefinite programming (SDP), it helps to review a simpler problem, namely that of linear programming (LP). The standard form of a linear program is [44]

$$
\begin{aligned}
\max\ & c^T x \\
& s.t. : \\
& Ax = b, \\
& x \geq 0,
\end{aligned}
\tag{171}
$$

with x being a vector of n variables, with all non-negative coefficients.

A set K is known as a closed convex cone if for any $x, \omega \in K$ and $\alpha, \beta \in \mathbb{R}^n_+$, then $\alpha x + \beta \omega \in K$, and K is a closed set.

The linear programming problem can thus be formulated as [21]: minimize the linear function $c^T \cdot x$, such that x solves the equations $A = b$, and x is in the convex cone K.

To the linear problem there corresponds a dual problem, a case which we will also encounter with semidefinite programs, later on. The dual can be formulated as

$$
\begin{aligned}
\min\ & b^T y \\
& s.t. : \\
& A^T y + s \geq c, \\
& s \geq 0,
\end{aligned}
\tag{172}
$$

Now we can compute the so-called duality gap simply as the difference between the two functions over which optimization is performed

$$c^T x - \sum_{i=1}^{m} y_i b_i = (c - \sum_{i=1}^{m} y_i a_i) x = sx \geq 0, \qquad (173)$$

since $x \geq 0$ and $s \geq 0$. From LP-duality theory, we know that, if the boundary is feasible and has a bounded optimal objective value (notions we shall discuss in detail for SDPs), the primal and dual both achieve their optima with zero duality gap. Thus, there exists x^*, and a pair (y^*, s^*) such that

$$c^T x^* - \sum_{i=1}^{m} y_i^* b_i = s^* x^* \geq 0. \qquad (174)$$

B.   Semidefinite Programming (SDP)

This section briefly overviews the convex optimization procedure known as semidefinite programming. The aim of semidefinite programming is to minimize a linear function under the constraint that an affine combination of symmetric matrices is positive semidefinite. This is a convex constraint including semidefinite programs (SDP for short) in the class of convex optimization problems. This overview is a short summary of the introduction to semidefinite programming found in Ref.[50]. Other resources discussing various aspects of SDPs in detail are Ref.[21, 44, 53].

An SDP can be formulated as the problem of minimizing a variable $x \in \mathbb{R}^m$ in the form

$$\begin{aligned}
& \min \ c^T x \\
& \text{s.t. :} \\
& F(x) = F_0 + \sum_{i=1}^{m} x_i F_i \\
& F(x) \geq 0.
\end{aligned} \qquad (175)$$

The vector $c \in \mathbb{R}^m$ and the $m+1$ symmetric matrices $F_0, ..., F_m \in \mathbb{R}^{nxn}$ represent the problem data, while the $F(x) \geq 0$ constraint means that $F(x)$ is a positive semidefinite matrix,

$$z^T F(x) z \geq 0, \qquad (176)$$

or, alternately, all eigenvalues of $F(x)$ are positive.

An SDP is a convex optimization problem since for $F(x) \geq 0$ and $F(y) \geq 0$, for all $\lambda \in [0, 1]$ we have

$$F(\lambda x + (1 - \lambda y)) = \lambda F(x) + (1 - \lambda)F(y) \geq 0, \qquad (177)$$

hence both the objective function and the constraint are convex.

It may prove useful to note that, since semidefinite programming can be regarded as an extension of linear programming, the linear problem described in Eq.(171) can be formulated as an SDP with the constraints

$$F_0 = \mathrm{diag}(b),$$
$$F_i = \mathrm{diag}(a_i), \qquad (178)$$

for all $i = 1...m$.

To the SDP one can then associate a dual semidefinite program (from now on it will be referred to as SDD) of the form

$$\mathrm{max} \quad -\mathrm{Tr}(F_0 Z)$$
$$s.t. :$$
$$\mathrm{Tr}(F_i Z) = c_i, \qquad (179)$$
$$Z \geq 0,$$

again, for all $i = 1...m$. In this case, the variable is the matrix $Z = Z^T \in \mathbb{R}^{n x n}$.

Hence forth we refer to the original SDP as the *primal problem* and to the SDD as the *dual problem*, and consider a matrix Z to be *dual feasible* if

$$\mathrm{Tr}(F_i Z) = c_i, \qquad (180)$$
$$Z \geq 0.$$

To go back to the previous example, the linear problem associated with $F_0 = \mathrm{diag}(b)$ and $F_i = \mathrm{diag}(a_i)$ can be associated with a dual of the form

$$\max \quad - \text{Tr}(\text{diag}(b)Z)$$

$$s.t. :$$

$$\text{Tr}(\text{diag}(a_i)Z) = c_i, \tag{181}$$

$$Z \geq 0,$$

with $i = 1...m$.

Due to the semidefinite constraint $Z \geq 0$ and the fact that the constraints involve diagonal elements of Z exclusively, this form of the SDD can be simplified by considering only Z matrices of diagonal form written as vectors $z = \text{diag}(Z)$, and the SDD becomes

$$\max \quad - b^T z$$

$$s.t. :$$

$$a_i^T z = c_i, \tag{182}$$

$$z \geq 0,$$

with $i = 1...m$.

One important property of SDPs and their associated duals is that one sets bounds on the optimal value of the other. If F is dual feasible and x is primal feasible, then the following always holds

$$c^T x + \text{Tr}(ZF_0) = \sum_{i=1}^{m} \text{Tr}(ZF_i x_i) + \text{Tr}(ZF_0) = \text{Tr}(ZF(x)) \geq 0, \tag{183}$$

because $\text{Tr}(AB) \geq 0$ if $A = A^T \geq 0$ and $B = B^T \geq 0$. This reduces to

$$- \text{Tr}(F_0 Z) \leq c^T x, \tag{184}$$

so the dual objective value of any dual feasible point Z is smaller than or equal to the primal objective value of any primal feasible point x.

With this, one can define the *duality gap* η as

$$\eta = c^T x + \text{Tr}(F_0 Z) = \text{Tr}(F(x)Z). \tag{185}$$

If α is the optimal value of the SDP

$$\alpha = \inf\{c^T x | F(x) \geq 0\}, \tag{186}$$

for any dual feasible Z and primal feasible x, then $- \operatorname{Tr}(ZF_0) \leq \alpha$. Analogously if β is the optimal value of the SDD,

$$\beta = \sup\{\operatorname{Tr}(F_0 Z) | Z = Z^T \geq 0, \quad \operatorname{Tr}(F_i Z) = c_i, \quad i = 1...m\}, \tag{187}$$

then $\beta \leq c^T x$. This is to be understood as dual feasible matrices imposing a lower bound on the primal problems and primal feasible points imposing an upper bound on the dual problem. What one generally sees is that, in practice, the rather strong condition $\alpha = \beta$ holds.

Theorem IV.1. *The condition $\alpha = \beta$ holds if any of the following requirements is true:*

- *The primal problem is strictly feasible, thus there exists x such that $F(x) \geq 0$.*

- *The dual problem is strictly feasible, thus there exists Z such that $Z = Z^T > 0$.*

For a proof of this theorem see Ref. [36].

C. Examples

Two examples of semidefinite programming applications in quantum information theory will be provided here. For more detail and implementations see Ref.[43].

Fidelity

Fidelity can be defined between two Hermitian positive-semidefinite operators P and Q, as

$$F(P,Q) = ||P^{1/2}Q^{1/2}|| = \max_U | \operatorname{Tr}(P^{1/2}UQ^{1/2})|. \tag{188}$$

This quantity can be expressed as an SDP

$$\max_{Z \in \mathcal{C}^{n \times n}} \frac{1}{2} \operatorname{Tr}(Z + Z^*)$$

$$s.t. :$$

$$\begin{pmatrix} P & Z \\ Z^* & Q \end{pmatrix} \geq 0 \tag{189}$$

Phase Recovery

Here, the main problem is to reconstruct the phase of a vector, about which we only know the magnitude of some linear measurements. Given a linear operator A and a vector b of measurement amplitudes, one can define a positive-semidefinite Hermitian matrix

$$M = \operatorname{diag}(b)(\mathbb{1} - AA^\dagger)\operatorname{diag}(b), \tag{190}$$

and formulate the Phase-cut problem as

$$\min_U \; \langle U, M \rangle$$

$$s.t. :$$

$$\operatorname{diag}(U) = 1 \tag{191}$$

$$U \geq 0,$$

where U must necessarily be Hermitian. This method was proposed in Ref.[51] and an implementation is given in Ref.[43].

66

V. Proving Genuine Multipartite Entanglement from Separable Nearest-Neighbour Marginals

A. Introduction

An essential property of quantum systems is that they can be entangled, meaning that the state of the system cannot be factorized. In the multipartite case, it is also interesting to ask what is the relationship between the global properties of the system and the local properties of its subsystems. This is a rather old problem, sometimes called the marginal problem, or the representability problem [16]. The notion that arises from this is *emergence*, the appearence of global properties which cannot be found in the subsystems. In the case of entanglement, the search is further motivated by the existence of entangled states with separable two-body marginals, where entanglement can be proven from the marginals alone. Such observations have been made in the context of spin squeezing [47, 48], and of Bell inequalities [49, 56], where the marginals are compatible with a local hidden-variable model, but the global state is not, and this can be proven from the marginals.

The question posed in the above papers was whether or not the global state can be factorized, thus if it is fully separable. In other words, if the state does not factorize, it is entangled, but not necessarily genuinely multipartite entangled. Thus the question of proving that a state is genuinely multipartite entangled just from separable two-body marginals still remained.

In [33], the authors have provided a method of detecting genuinely multipartite entangled states, with separable two-body marginals, where entanglement can be proven from the marginals only. They have also provided a scheme for constructing states with the desired properties for any number of particles, and gave examples of numerically found states for up to five particles.

Our aim here is to go one step further and see what happens when only nearest-neighbour marginal information is known, still all marginals are separable. We will see that it is possible, although white-noise tolerance suffers strongly, that one can prove the genuine multipartite entangledness of the global state just from separable two-body nearest-neighbour marginals only. We were able to go as high as six qubits, for various configurations. In Fig. 18 we present the useful configurations for five qubits, excluding cases in which parties are not connected or

FIG. 18: All possible tree configurations of known marginals for 5 qubits.

cases where non-neighbouring parties are connected. In the latter part of the paper, we present a method of constructing higher-dimensional states, using copies of the numerically found five and six qubit states.

B. Implementation

To obtain an optimal state, with the desired properties, we implement our program as a sequence of steps, over which an iteration is performed, until the desired precision is reached.

Step 0: Generate a quasi-random pure state ρ. By quasi-random we just mean the state should not have too much symmetry, a random matrix generated with the Python random package suffices for this.

Step 1: Insert the state into the first semidefinite program (SDP). The point of this program is to find an optimal witness, that has the smallest expectation value possible, with

respect to the given state. Formally, one writes this program as

$$\min \operatorname{Tr}(W\rho)$$

$$s.t.:$$

$$\operatorname{Tr}(W) = 1$$

$$W = \sum_{i,j}\sum_{k=0}^{N-2} \omega_{i,j} \mathbb{1}^{\otimes k} \sigma_i^{\alpha} \otimes \sigma_j^{\beta} \otimes \mathbb{1}^{\otimes(N-2-k)} \tag{192}$$

$$W = P_M + Q_M^{T_M} \qquad P_M, Q_M \geq 0$$

The first condition, $Tr(W) = 1$ is just a normalization condition on the witness. While the witness parametrization we chose here ($\operatorname{Tr}(W) = 1$) is not the only possible one, it does however assure the best noise robustness. The permutations in the second condition are taken only over nearest-neighbour marginals. The second condition tells the program that the witness only has information about nearest-neighbour marginals, while the last condition ensures that the witness is fully decomposable, hence it can detect non-PPT mixtures.

Step 2: Insert the optimal witness, from the previous step, into a second SDP, whose purpose is to obtain an optimal state, that minimizes the expectation value of W as much as possible. This program is

$$\min \operatorname{Tr}(W\rho)$$

$$s.t.:$$

$$Tr(\rho) = 1 \tag{193}$$

$$\rho \geq 0$$

$$\rho_{\alpha,\beta}^{T_{\alpha}} \geq 0 \ \forall \alpha, \beta$$

While the first two conditions are present just to assure the fact that ρ is still a density matrix, the third one represents the constraint that all marginals of ρ must be separable (not just the nearest-neighbour ones).

One can now repeat the iteration between steps 1 and 2, obtaining a better approximation of an optimal state with each additional step.

In practice, the two SDPs have been implemented in Python, using the Picos [43] convex optimization interface. After a remarkably small number of iterations (usually 2 or 3), one would already find a state that satisfies the desired requirements. On a regular desktop

configuration, the four qubit state is obtained in under a minute, the five qubit state in around 45 minutes and the six qubit state in around 6 hours. We thus managed to obtain such states for four, five and six qubits, for various configurations (see Fig.18). We started with a pure initial quasi-random state, and it's important to mention that all optimal states are also pure, except for one, the four-qubit linear state (equivalent to the top configuration in Fig.18). The obtained states are also uniquely determined, that is, the corresponding smallest eigenvalue of the witness is non-degenerate. This will prove to be essential later on, when we discuss generalizations of these results.

C.   Results

In this section, we present the results obtained by using the previously described method. The starting point is a randomly generated pure state. This state is passed through the SDP from Step 1, and an optimal witness is obtained. Among the constraints imposed on the witness is that it is fully decomposable and that only information about nearest-neighbour two-body marginals is known. This witness is then passed through the second SDP, described in Step 2, and we obtain a state which provides a maximal violation of the witness, while under the constraint that all its two-body marginals are separable (equivalent to PPT in this case). Finally, this state is again passed through the first SDP (Step 1). After a small number of cycles, a state is obtained, satisfying the condition that, even though all its two body marginals are separable (from the constraint at Step 2), one can still prove the state is genuinely multipartite entangled by knowing the two-body nearest-neighbour marginals only (second constraint imposed at Step 1).

1.   Four Qubits

There are two possible configurations for four qubits, a linear state, and a half-star shaped state (the interaction of one particle with the other three being known). While for both configurations we obtained genuinely multipartite entangled states with the desired requirements, the linear state is not pure. We show here the other state, which is pure and uniquely

70

determined by its nearest-neighbour two-body marginals.

$$|\psi_4\rangle = \frac{1}{\sqrt{87}}(5\,|\phi_1\rangle + \sqrt{10}\,|\phi_2\rangle + \sqrt{3}\,|\phi_3\rangle + 7\,|\phi_4\rangle) \tag{194}$$

where the component states are

$$|\phi_1\rangle = \frac{1}{\sqrt{2}}(e^{\frac{3\pi}{7}i}\,|1100\rangle - |0000\rangle)$$

$$|\phi_2\rangle = \frac{1}{\sqrt{5}}(e^{\frac{\pi}{4}i}\,|0101\rangle - |0111\rangle - |1000\rangle - |1001\rangle - |1111\rangle)$$

$$|\phi_3\rangle = \frac{1}{\sqrt{6}}(e^{\frac{-2\pi}{3}i}\,|0010\rangle + |0011\rangle + |0100\rangle + |1010\rangle$$

$$+ |1101\rangle + |1110\rangle)$$

$$|\phi_4\rangle = \frac{1}{\sqrt{2}}(|0110\rangle - |1011\rangle)$$

This is the closest analytical state to the one obtained numerically. The white noise tolerance of the numerical state is 0.35%.

2. Five Qubits

We show here the linear five qubit state. There are three possible configurations, in which only nearest-neighbour information is known (Fig.18). This state is pure and uniquely determined.

$$|\psi_5\rangle = \frac{1}{\alpha}(\frac{1}{4}\,|\phi\rangle + \frac{3}{2}\sqrt{\frac{3}{10}}\,|\eta\rangle + \frac{1}{14}e^{\frac{2\pi i}{3}}\,|11101\rangle$$

$$+ \frac{2}{11}e^{\frac{-3\pi i}{13}}\,|11111\rangle) \tag{195}$$

71

where the corresponding substates are

$$|\eta\rangle = \sqrt{\frac{2}{15}}(\frac{\sqrt{6}}{2}|\eta_1\rangle + \sqrt{2}|\eta_2\rangle - 2|\eta_3\rangle)$$

$$|\eta_1\rangle = \sqrt{\frac{1}{6}}(|00011\rangle - |00001\rangle - |01001\rangle + |01010\rangle$$
$$- |10000\rangle + |10011\rangle))$$

$$|\eta_2\rangle = \frac{1}{3\sqrt{2}}(e^{\frac{\pi i}{8}}|01100\rangle + e^{\frac{\pi i}{8}}|11001\rangle + 4|11110\rangle)$$

$$|\eta_3\rangle = \frac{1}{2}(|11010\rangle + |11100\rangle + |11000\rangle + |00000\rangle)$$

$$|\phi\rangle = \frac{1}{\beta}(\frac{1}{2}|\phi_1\rangle + \frac{\sqrt{2}}{3}e^{\frac{\pi i}{4}}|\phi_2\rangle + \frac{\sqrt{3}}{5}|\phi_3\rangle + 2|\phi_4\rangle)$$

$$|\phi_1\rangle = \frac{1}{2}(e^{\frac{\pi i}{4}}|00010\rangle - \frac{1}{2}|01011\rangle - \frac{1}{2}|01101\rangle$$
$$+ |01110\rangle - \frac{1}{2}|01111\rangle - \frac{1}{2}|10111\rangle + |11011\rangle)$$

$$|\phi_2\rangle = \frac{1}{\sqrt{2}}(|00110\rangle + |01000\rangle)$$

$$|\phi_3\rangle = \frac{1}{\sqrt{3}}(|00100\rangle + |00101\rangle + |10101\rangle)$$

$$|\phi_4\rangle = \frac{1}{2}(|10010\rangle + |10100\rangle + |10110\rangle - |10001\rangle)$$

Here, α and β are two normalization constants which have been left out, for clarity. Due to the severe limitation on the information regarding the marginals, the state has very low noise robustness (around 0.11%), but the entanglement of the global state can be proven from the separable nearest-neighbor marginals only.

3. Six Qubits

In this case, there are four possible nearest-neighbor configurations and, like in the five qubit situation, they are all pure and uniquely determined. Due to its size, we present the state in numeric form, in Appendix A1, up to some normalization coefficient.

It is important to also mention that noise tolerance for the numerical six qubit state is approximately 0.02%, and the expectation value of the optimal witness, together with this state, while negative, is of the order of 10^{-4}. All configurations for nearest-neighbour marginals that have been tested are presented in Table III (Appendix A1).

D. Generalization

The purpose of this last section is to prove that one could use the states found so far, in order to construct states, of much larger systems, with the same properties. The downside to this generalization, however, is that one must resort to higher dimensional systems, where each party does not consist of only a qubit. The state we use here to exemplify is the linear five qubit state. The first example is for a simple six-party system, depicted in Fig.19.

The state we want to construct is $|\theta\rangle$. The parties A and F have a single qubit while the ones from B to E have two qubits. We depict the two-party marginals by blue lines. All we need to do is to distribute two copies of the pure five qubit state, represented by the thick red lines, (the state $|\psi_5\rangle$ in Eq.(195)) among the six parties.

Every two-party marginal is a direct product of separable states, thus it is itself separable. Due to the fact that $|\psi_5\rangle$ is uniquely determined by its two-body nearest-neighbour marginals, if one knows the marginals, one also knows the state $|\psi_5\rangle$ and the way copies of this state have been distributed among the parties. This also means that the global state itself, namely $|\theta\rangle$, is uniquely determined by its two-body nearest-neighbour marginals as well.

The constructed state is also pure and cannot be factorized for any bipartition of the system, so it clearly is genuinely multipartite entangled, and this entanglement is proven from the nearest-neighbor two-body marginals only, since the constructed state is just made up of copies of $|\psi_5\rangle$.

One remark that must be made in this case is that it's essential that the linear five-qubit state we're using here be uniquely determined by its marginals, and this has been tested for all numerically obtained states and found to be true.

If we consider a 4×4 two-dimensional lattice, as depicted in Fig.20, it can be fully covered by using four copies of the linear five-qubit state. Nodes H, I, L and P contain two qubits, one from each copy of the state, so we require a total of 20 qubits to construct the desired lattice state.

Now we try the same procedure for an arbitrary configuration. Consider the ten parties (A to J) in Fig.21. Each of the parties has at least one qubit (H and J) and at most three (C and F). By repeating the same algorithm as above, and distributing as few copies of the five-qubit state as possible, while still covering every party by at least one copy, we obtain a
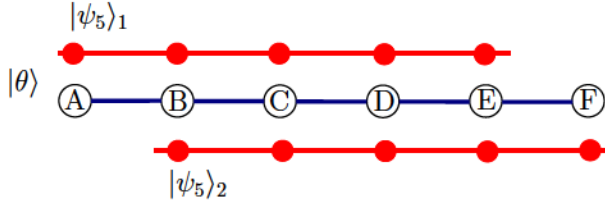
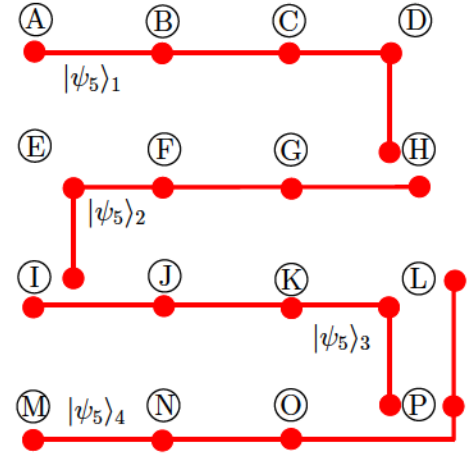FIG. 19: Constructing a state with the desired properties for a simple six-party configuration.

FIG. 20: Covering a two-dimensional lattice with linear numerically-found states.

ten-particle state, with the same properties as the one above.

One could start here by using a large number of copies, in a non-optimal situation, making sure that two states cover just one two-party marginal. This would thus mean throwing away a large number of qubits, and still be able to construct the desired state. Again the fact that the underlying numerically obtained states are pure and uniquely determined is essential.

Due to the fact that, with our semidefinite program, we were able to go as high as six qubits, one could take advantage of this and use the linear six-qubit state instead. While less robust to noise, an arbitrary configuration would require less copies of the state, thus helping to reduce de dimensionality of some of the systems (for example C and F in Fig.21 are three-qubit systems).

The fact that one can create these states for very large systems, and still manage to prove the entanglement from nearest-neighbour marginals only must be stressed.

While in our work, we only looked at two-body marginals, the problem could be taken one step further by also treating higher order marginals and proving the genuine multipartite entanglement of the global state just with the knowledge of those marginals. This would, however, require more information about the state.

As a final remark, the states presented here have a rather low noise tolerance (for example 0.02% for the six qubit state), and it decreases with the increase in the number of qubits. This is mainly due to the strong constraint on nearest-neighbour information only. Nevertheless
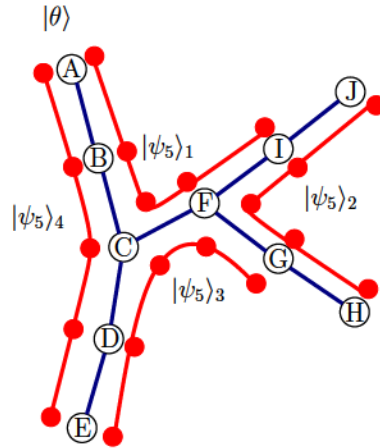
FIG. 21: Constructing a state with the desired properties for an arbitrary configuration.

it would be interesting to see an experimental study of the effects discussed here.

1. Summary

In this second part we presented our work on the problem of detecting genuine multipartite entanglement for states with separable two-body marginals. This is an optimization problem that can be conveniently formulated in terms of two semidefinite programs. The details of the implementation are given in Appendix A2. By gradually increasing the size of the system and applying iteratively the two programs, we managed to obtain states with the desired properties for four, five and six qubits. Remarkably, all states are pure, except for the four qubit linear state (see. Appendix A1), and all are uniquely determined by their nearest-neighbour two-body marginals. Taking advantage of these properties, we also provided a way to construct arbitrarily large quantum states, by using multiple copies of the numerically found ones, and retaining the same entanglement properties.

VI. Conclusion

This thesis brings together our approach to two problems in the study of quantum entanglement. In the first part we addressed the question of entanglement loss in an open system while in the second, the appearance of genuine multipartite entanglement in a multiparticle system where the reduced states are not entangled.

While considering a specific unstable particle, we expanded on an already-existing effective formalism and obtained a generalization, applicable to any multilevel quantum system. This provides the means to test the loss of entanglement in a system in contact with an environment, in a very broad sense, without the need to consider the environment's degrees of freedom. More specifically, in the case of neutral kaons, the exact decay product states for every event need not be specified, in order to test the presence of entanglement between the particle-antiparticle pair. Due to the normalization procedure that includes decay products, one can observe entanglement for a time comparable to the lifetime of the short-lived kaon state. Finally, we provided two experimental examples of how this generalized formalism could be used in practice, to study entanglement by using trapped ions.

The usage of the effective formalism can be further expanded by considering an arbitrarily high number of levels and population decay also inside the system (between levels that are not part of the environment). For a better understanding of the effect of improper state preparation or noise, one could artificially introduce behaviours similar to CP-violaion and particle oscillation.

In the second part of the thesis, the question of entanglement as an emergent phenomenon has been considered. By imposing the constraints that a desired multiparticle state should have separable two-body marginals, but the global state should be genuinely multipartite entangled, we managed to numerically find states satisfying these conditions. Furthermore we proved the entanglement of the global state only from a known subset of nearest-neighbour two-body marginals. In the end we provided a means of constructing arbitrarily large states with the same properties, by using the numerically-found ones as building blocks.

Though we only considered two-body marginals in our work, it would be interesting to see genuine multipartite entanglement proven from larger subsystems as well. This would, however require more information about the global state.

We present here the numerical form of the four qubit state, from Section D.1.

$$|\psi_4\rangle = \frac{1}{N}\Bigg(-\frac{2}{33}+\frac{5i}{38},\ \frac{1}{21}+\frac{2i}{13},\ \frac{50}{149}+\frac{3i}{35},\ -\frac{1}{17}+\frac{3i}{25},\ \frac{7}{26}-\frac{5i}{28},\ -\frac{3}{32}+\frac{10i}{61},\ \frac{7}{62}+\frac{6i}{17},$$
$$-\frac{2}{17}+\frac{i}{111},\ \frac{5}{23}+\frac{8i}{29},\ \frac{3}{31}+\frac{5i}{41},\ \frac{2}{41}-\frac{5i}{34},\ -\frac{1}{13}+\frac{11i}{30},\ -\frac{1}{289}+\frac{i}{51},$$
$$-\frac{1}{270}+\frac{i}{24},\ -\frac{1}{58}+\frac{7i}{24},\ \frac{11}{31}\Bigg)$$

Also, the numerical form of the five qubit state, presented in Section D.2.

$$|\psi_5\rangle = \frac{1}{N}\Bigg(-\frac{3}{35}-\frac{i}{22},\ \frac{4}{31}+\frac{i}{40},\ \frac{4}{29}-\frac{i}{22},\ -\frac{1}{28}+\frac{4i}{29},\ \frac{4}{35}-\frac{2i}{25},\ -\frac{1}{24}+\frac{i}{19},\ -\frac{6}{35}-\frac{5i}{28},$$
$$\frac{2}{33}-\frac{4i}{45},\ \frac{1}{32}-\frac{i}{3},\ \frac{3}{35}-\frac{19i}{94},\ -\frac{5}{24}-\frac{3i}{16},\ \frac{1}{74}-\frac{2i}{33},\ -\frac{4}{27}+\frac{i}{207},\ -\frac{1}{186}-\frac{2i}{39},$$
$$\frac{5}{41}-\frac{2i}{13},\ \frac{2}{19}+\frac{5i}{34},\ -\frac{2}{27}+\frac{i}{6},\ -\frac{3}{29}-\frac{8i}{33},\ -\frac{1}{8}-\frac{5i}{36},\ \frac{7}{30}-\frac{3i}{40},\ -\frac{4}{31}-\frac{5i}{28},$$
$$\frac{1}{7}-\frac{3i}{35},\ -\frac{11}{36}+\frac{i}{83},\ \frac{1}{50}-\frac{2i}{35},\ \frac{1}{10}-\frac{8i}{41},\ \frac{1}{26}-\frac{i}{50},\ -\frac{4}{39}-\frac{2i}{29},\ -\frac{2}{29}-\frac{2i}{19},$$
$$-\frac{1}{18}-\frac{i}{295},\ -\frac{2}{27}-\frac{2i}{23},\ -\frac{1}{18}-\frac{4i}{33},\ \frac{1}{10}\Bigg)$$

Due to its size, we only present the linear six qubit state in numerical form, up to some normalization factor.

$$|\psi_6\rangle = \frac{1}{N}\Bigg(\frac{3}{77},\ 0,\ \frac{1}{55},\ -\frac{4}{61}-\frac{6i}{85},\ -\frac{2}{97},\ 0,\ 0,\ \frac{3}{107},\ -\frac{10}{59},\ \frac{1}{133}-\frac{7i}{167},\ -\frac{7}{211},\ -\frac{7}{211},$$
$$-\frac{1}{27}+\frac{21i}{106},\ -\frac{23}{172}-\frac{6i}{121},\ -\frac{11}{70},\ \frac{1}{106}-\frac{8i}{193},\ -\frac{7}{211},\ \frac{9}{167},\ \frac{13}{168},\ -\frac{33}{97},$$
$$\frac{10}{103}+\frac{17i}{77},\ \frac{13}{168},\ \frac{8}{61},\ \frac{8}{83},\ \frac{16}{43},\ 0,\ \frac{1}{128}-\frac{11i}{84},\ \frac{29}{83},\ 0,\ \frac{47}{168},\ \frac{16}{43},\ \frac{9}{167},\ 0,\ 0,$$
$$-\frac{1}{117},\ -\frac{17}{358}+\frac{15i}{188},\ -\frac{1}{79}+\frac{10i}{191},\ 0,\ 0,\ -\frac{7}{181}+\frac{i}{25},\ \frac{2}{63}+\frac{9i}{103},\ 0,\ 0,\ \frac{10}{91},$$
$$\frac{5}{127}+\frac{9i}{79},\ 0,\ \frac{2}{59}+\frac{5i}{72},\ -\frac{3}{137},\ -\frac{3}{107},\ -\frac{6}{161}+\frac{4i}{59},\ -\frac{8}{159}+\frac{4i}{93},\ \frac{28}{159}+\frac{29i}{217},$$
$$-\frac{3}{137},\ -\frac{3}{107},\ -\frac{3}{107},\ -\frac{5}{62}+\frac{2i}{17},\ \frac{3}{137},\ 0,\ \frac{3}{137},\ -\frac{3}{107},\ -\frac{2}{43}-\frac{7i}{87},\ \frac{1}{174},$$
$$0,\ -\frac{3}{65}+\frac{6i}{125}\Bigg)$$

This state is also pure and uniquely determined by its two-body nearest-neighbour marginals, while still retaining the desired properties, namely the state should be genuinely multipartite entangled and the entanglement should be proven from the separable nearest-neighbour two-body marginals only.
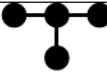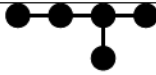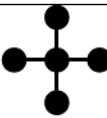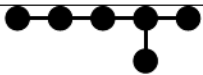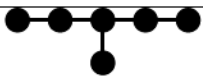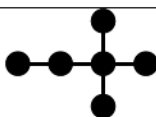
Configuration	$\mathrm{Tr}[\rho W]$	Pure
4-Qubit Configurations		
	$-3.15 \cdot 10^{-3}$	No
	$-3.56 \cdot 10^{-3}$	Yes
5-Qubit Configurations		
	$-1.13 \cdot 10^{-3}$	Yes
	$-1.31 \cdot 10^{-3}$	Yes
	$-1.38 \cdot 10^{-3}$	Yes
6-Qubit Configurations		
	$-2.01 \cdot 10^{-4}$	Yes
	$-2.56 \cdot 10^{-4}$	Yes
	$-2.92 \cdot 10^{-4}$	Yes
	$-3.80 \cdot 10^{-4}$	Yes

TABLE III: Tested states with various configurations. All states are uniquely determined by their known two-body nearest-neighbour marginals.

We provide here a detailed description of our implementation of the two semidefinite problems. The two main Python 2.7 modules used were numpy and cvxopt, for basic numerical operations and convex optimization. To greatly simplify the code, we used a python wrapper called Picos [43] which also helps with code readability. Finally, the solver we decided to use is mosek7, chosen for its much faster runtimes, compared with regular open-source solvers, such as cvx and dsdp.

The problem of finding genuinely multipartite entangled states with separable two-body nearest-neighbour marginals was split into two SDPs, a "state solver", whose role was to find an optimal state ρ for a given witness W, and a "witness solver" which provided an optimal witness for a given state (with which the given state would obtain maximal violation).

An example of state solver for 3 qubits (for brevity) is given here.

```python
def State_Solver(n,W):
    P = pic.Problem()

    Rho = P.add_variable('Rho',(n,n),'hermitian')
    W   = pic.new_param('W', W)

    P.add_constraint(pic.trace(Rho)==1)
    P.add_constraint(Rho >> 0)

    P.add_constraint(pic.partial_transpose(pic.partial_trace(Rho
    ,0,(2,2,2))) >>0)
    P.add_constraint(pic.partial_transpose(pic.partial_trace(Rho
    ,1,(2,2,2))) >>0)
    P.add_constraint(pic.partial_transpose(pic.partial_trace(Rho
    ,2,(2,2,2))) >>0)

    P.set_objective('min',(Rho|W))
```

```
15        sol = P.solve(solver='mosek7',verbose=False)

16

17        Rho_ARM = np.array(Rho.value)

18        return Rho_ARM
```

Lines 2-5 initialize the picos problem and define the variable Rho and parameter W. The states and witnesses are stored in csv files and imported into the main program when needed. The constraints upon the state are enforced in lines 7-12, both to ensure that Rho is still a valid quantum state and that its three possible two-body marginals are separable (condition imposed here through the fact that the partial transpose of Rho should be positive semidefinite). Lines 14-18 set the objective of the problem as minimizing the trace of Rho and W, choose mosek7 as the solver and return Rho as a numpy array. Unfortunately, at the time when the code was written, the partial transpose and partial trace functions were not properly implemented in Picos, such that the rather cumbersome function nesting had to be used in the constraints.

The program for witness optimization is somewhat similar.

```
1 def Witness_Optimizer(n,interact_basis,state):
2        P = pic.Problem()
3        Rho = pic.new_param('Rho',state)
4        I = pic.new_param('I',cvx.matrix(np.eye(8)))
5
6        W = P.add_variable('W',(n,n),'hermitian')
7        Q1 = P.add_variable('Q1',(n,n),'hermitian')
8        Q2 = P.add_variable('Q2',(n,n),'hermitian')
9        Q3 = P.add_variable('Q3',(n,n),'hermitian')
10
11
12        P.add_constraint(pic.trace(W)==1)
13
14        P.add_constraint(Q1 >> 0)
15        P.add_constraint(Q2 >> 0)
```

```
16      P. add_constraint (Q3 >> 0)

17

18      P. add_constraint ((W − pic . partial_transpose (Q1,(2,2))) >> 0)

19      P. add_constraint ((W − pic . partial_transpose (pic . partial_transpose (
        Q2,(4,4)),(2,2))) >> 0)

20      P. add_constraint ((W − pic . partial_transpose (pic . partial_transpose (
        Q3,(8,8)),(4,4))) >> 0)

21

22      P. set_objective ('min',(Rho|W))

23

24      P. solve (solver='mosek7', verbose=False)

25

26      return  np. array (W. value)
```

Since we are considering a fully decomposable witness $W = P_M + Q_M^{T_M}$, we need three extra parameters, defined in lines 7-9. The fact that we require the trace of W to be equal to one and that $P_M \geq 0$ and $Q_M \geq 0$ result in the conditions from lines 12-20.

If one wishes for the witness to contain only information about the nearest neighbour marginals, one can simply impose the condition that

$$\mathrm{Tr}[W\sigma \otimes \sigma \otimes \sigma] = 0,$$

where $\sigma \otimes \sigma \otimes \sigma$ stand for all permutations of Pauli matrices and identity matrices, excluding the basis that one is interested in (for example $\sigma_x \otimes \sigma_x \otimes \mathbb{1}$).

Finally, a remark about the running time. Even though it is highly dependent on the hardware configuration, on a typical desktop computer the four qubit programs ran for around 15 minutes, the five qubit configurations took close to four hours and the six qubit configurations required roughly one full day of runtime.
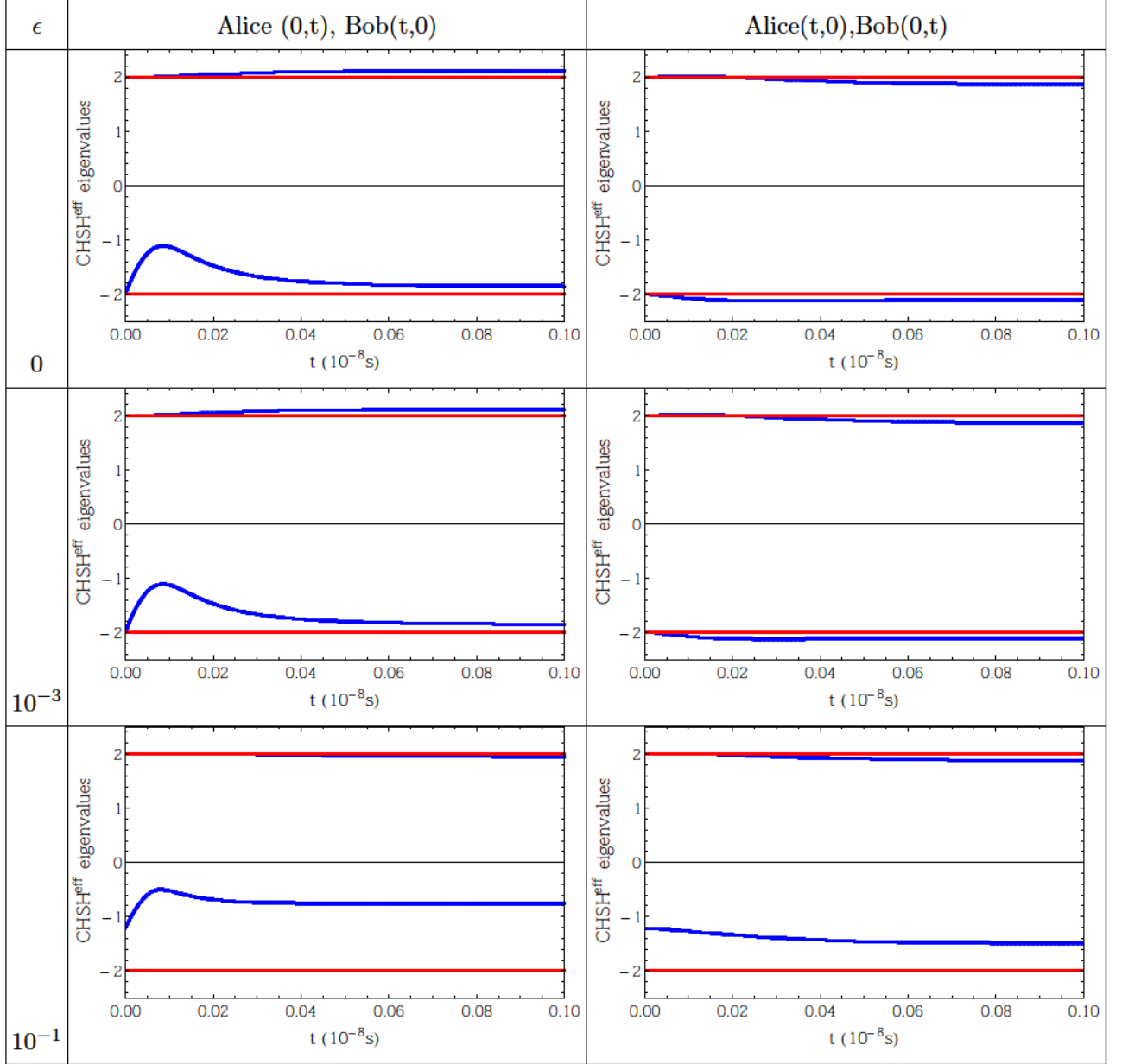
TABLE IV: Plots (for neutral kaons) for the minimal and maximal eigenvalues of the CHSH effective operator, represented here in blue (dark gray), for certain values of the CP-violation parameter. The red (light gray) lines represent the classical limits of the CHSH inequality. The settings are for both Alice and Bob measuring at different times, for example A(0,t) means Alice's first measurement is made at $\tau = 0$ and the second measurement at $\tau = t$, where t is a plot parameter.

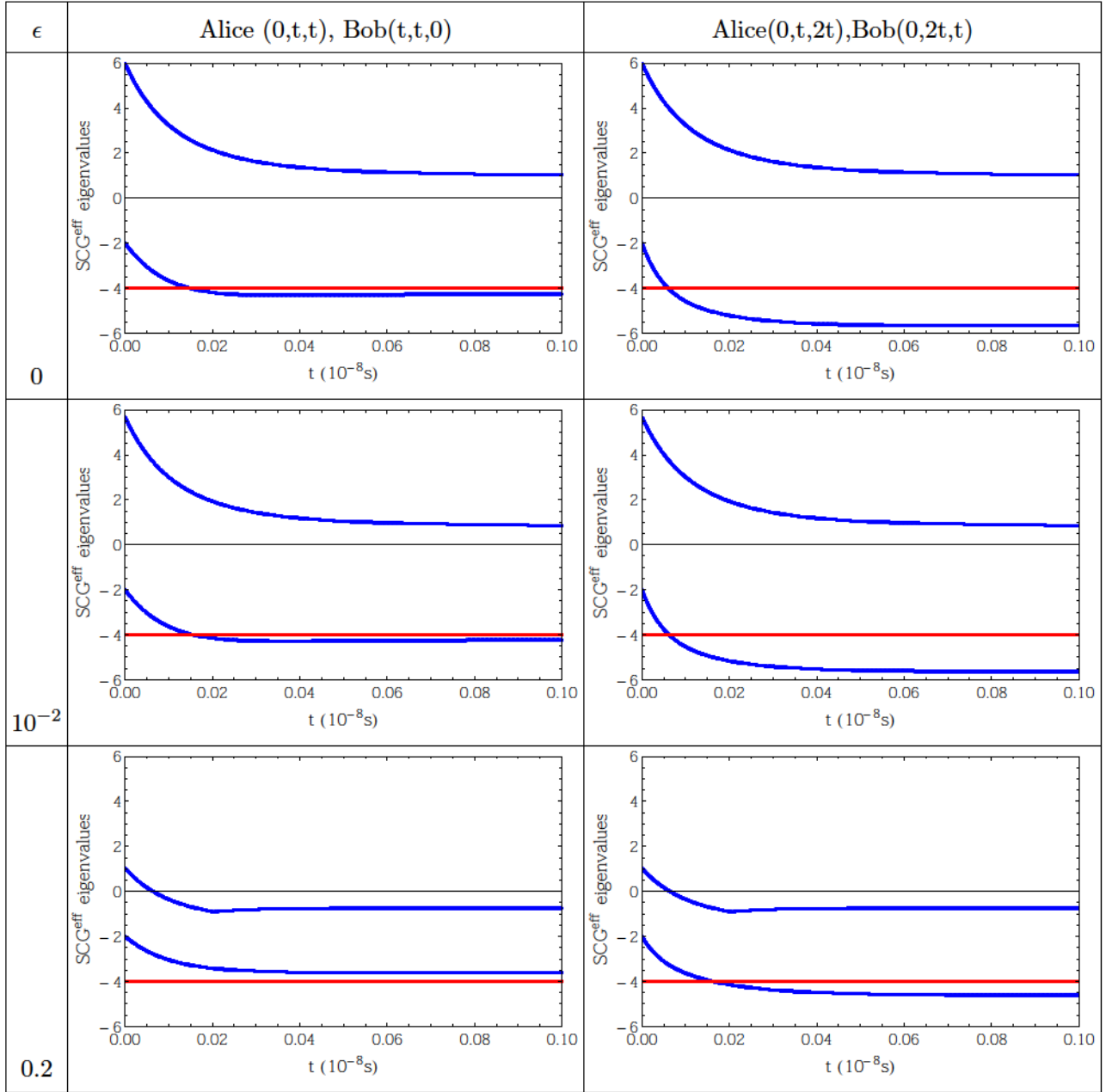| ϵ	Alice (0,t,t), Bob(t,t,0)	Alice(0,t,2t),Bob(0,2t,t)
0		
10^{-2}		
0.2		

TABLE V: Plots (for neutral kaons) for the minimal and maximal eigenvalues of the SCG effective operator, represented here in blue (dark gray), for certain values of the CP-violation parameter. The red (light gray) line represents the classical limit of the SCG inequality.

References

[1] AULETTA, G., FORTUNATO, M., AND PARISI, G. *Quantum Mechanics*. Cambridge University Press, 2009.

[2] BELL, J. S. On the Einstein Podolsky Rosen Paradox. *Physics 1* (1964), 195–200.

[3] BENNETT, C., AND BRASSARD, G. Quantum Cryptography: Public Key Distribution and Coin Tossing. In *Proceedings IEEE International Conference on Computer Systems, New York* (1984), pp. 175–179.

[4] BERTLMANN, R. A. Entanglement, Bell Inequalities and Decoherence in Particle Physics . *Lect. Notes Phys.*, 689 (2006), 1–45.

[5] BERTLMANN, R. A., BRAMON, A., GARBARINO, G., AND HIESMAYR, B. C. Violation of a Bell inequality in particle physics experimentally verified? . *Phys. Lett. A 332*, 5-6 (2004), 355–360.

[6] BLOCH, F. Nuclear Induction . *Phys. Rev. 70*, 460 (1946).

[7] BOHR, N. Can Quantum-Mechanical Description of Physical Reality be Considered Complete? . *Phys. Rev. 48*, 696 (1935).

[8] BRAMON, A., GARBARINO, G., AND HIESMAYR, B. C. Active and passive quantum erasers for neutral kaons . *Phys. Rev. A 69* (2004), 062111.

[9] BRASIL, C. A., FANCHINI, F. F., AND NAPOLITANO, R. A simple derivation of the Lindblad equation . *Rev. Bras. Ensino Fís. 35*, 1-6 (2013).

[10] BREUER, H. P., AND PETRUCCIONE, F. *The Theory of Open Quantum Systems*. Oxford University Press, 2010.

[11] CHRISTENSON, J. H., CRONIN, J. W., FITCH, V. L., AND TURLAY, R. Evidence for the 2π Decay of the K_2^0 Meson. *Phys. Rev. Lett. 13*, 138 (1964).

[12] CIREL'SON, B. S. Quantum generalizations of Bell's inequality. *Lett. Math. Phys. 93* (1980).

[13] CLAUSER, J. F., AND HORNE, M. A. Experimental consequences of objective local theories. *Phys. Rev. D 10* (1974), 526.

[14] CLAUSER, J. F., HORNE, M. A., SHIMONY, A., AND HOLT, R. A. Proposed experiment to test local hidden-variable theories. *Phys. Rev. Lett. 23* (1969), 880.

[15] CLAUSER, J. F., HORNE, M. A., SHIMONY, A., AND HOLT, R. A. Erratum : Proposed

experiment to test local hidden-variable theories. *Phys. Rev. Lett. 24* (1970), 549(E).

[16] COLEMAN, A. J. Structure of Fermion Density Matrices . *Rev. Mod. Phys. 35* (1963), 668.

[17] COLLINS, D., AND GISIN, N. A relevant two qubit Bell inequality inequivalent to the CHSH inequality. *J. Phys. A : Math. Gen. 37* (2004), 1775–1787.

[18] DOMENICO, A. D. E. A. Heisenberg's Uncertainty Relation and Bell Inequalities in High Energy Physics. *Found. Phys. 42*, 6 (2011), 778–802.

[19] EINSTEIN, A., PODOLSKY, B., AND ROSEN, N. Can Quantum-Mechanical Description of Physical Reality Be Considered Complete? *Phys. Rev. 47* (1935), 777.

[20] ESCHNER, J. Quantum computation with trapped ions. Proceedings of the International School of Physics 'Enrico Fermi' Course CLXII. `https://www.icfo.es/images/publications/Proc.06-002.pdf`.

[21] FREUND, R. M. Semidefinite Programming - Lecture Notes., 2009. `http://ocw.mit.edu/courses/electrical-engineering-and-computer-science/6-251j-introduction-to-mathematical-programming-fall-2009/readings/MIT6\_251JF09\_SDP.pdf`.

[22] GISIN, N., AND GO, A. EPR test with photons and kaons: Analogies . *Am. J. Phys. 69*, 264 (2001).

[23] GO, A. Observation of Bell inequality violation in B mesons . *J. Mod. Opt. 51*, 6-7 (2004), 991–998.

[24] GÜHNE, O., AND TÓTH, G. Entanglement Detection. *Physics Reports 474*, 1-6 (2009), 1–75.

[25] HORODECKI, M., HORODECKI, P., AND HORODECKI, R. Separability of mixed states: Necessary and sufficient conditions. . *Phys. Lett. A 1* (1996), 223.

[26] HORODECKI, R., HORODECKI, P., HORODECKI, M., AND HORODECKI, K. Quantum entanglement . *Rev. Mod. Phys. 81*, 865 (2009).

[27] `http://hyperphysics.phy-astr.gsu.edu/hbase/particles/cronin.html`.

[28] JOHANNING, M., BRAUN, A., TIMONEY, N., ELMAN, V., NEUHAUSER, W., AND WUNDERLICH, C. Individual Addressing of Trapped Ions and Coupling of Motional and Spin States Using rf Radiation . *Phys. Rev. Lett. 102* (2009), 073004.

[29] JUNGNITSCH, B., MORODER, T., AND GÜHNE, O. Taming Multiparticle Entanglement. *Phys. Rev. Lett. 106* (2011), 190502.

[30] LANYON, B. P., ET AL. Universal digital quantum simulation with trapped ions . *Science 57* (2011), 334.

[31] LEGGETT, A. J. Nonlocal hidden-variable theories and quantum mechanics: An incompatibility theorem. . *Found. Phys. 33* (2003), 1469.

[32] LEIBFRIED, D., BLATT, R., MONROE, C., AND WINELAND, D. Quantum dynamics of single trapped ions. *Rev. Mod. Phys. 75*, 1-6 (2003).

[33] MIKLIN, N., MORODER, T., AND GÜHNE, O. Multiparticle entanglement as an emergent phenomenon . *Phys. Rev. A 93* (2016), 020104(R).

[34] MINTERT, F., AND WUNDERLICH, C. Ion-Trap Quantum Logic Using Long-Wavelength Radiation . *Phys. Rev. Lett. 87* (2001), 257904.

[35] NAZIR, A. *Lecture notes on open quantum systems* . `https://workspace.imperial.ac.uk/people/Public/anazir1/open\_systems\_notes.pdf`.

[36] NESTEROV, Y., AND NEMIROVSKY, A. Interior-point polynomial methods in convex programming. *Studies in Applied Mathematics 13* (1994).

[37] NIELSEN, M. A., AND CHUANG, I. L. *Quantum Computation and Quantum Information.* Cambridge University Press, 2010.

[38] PARASCHIV, M., WÖLK, S., MANNEL, T., AND GÜHNE, O. Generalized Effective Operator Formalism for Decaying Systems . *arXiv:1607.00797*.

[39] PAUL, W. Electromagnetic traps for charged and neutral particles . *Rev. Mod. Phys. 62*, 531.

[40] PEARLE, P. Simple Derivation of the Lindblad Equation. *Eur. J. Phys. 33*, 4 (2012).

[41] PERES, A. Separability criterion for density matrices. *Phys. Rev. Lett. 77* (1996), 1413.

[42] PERES, A. All the Bell inequalities. *Found. Phys. 29* (1999), 589.

[43] SAGNOL, G. PICOS: A Python Interface for Conic Optimization Solvers. `http://picos.zib.de/index.html`.

[44] SAGNOL, G. Semidefinite Programming - Lecture Notes., 2014. `www.zib.de/sagnol/vorlesungen/optdes/SS14-OD-VL-08.pdf`.

[45] SCHALLER, G. Open Quantum Systems Far from Equilibrium . In *Lecture Notes in Physics 881*. Springer International Publishing Switzerland, 2014.

[46] SLIWA, C. Symmetries of the Bell correlation inequalities. *Phys. Lett. A 317* (2003), 165–168.

[47] TÓTH, G. Entanglement witnesses in spin models . *Phys. Rev. A 71*, 010301(R) (2005).

[48] TÓTH, G., KNAPP, C., GÜHNE, O., AND BRIEGEL, H. J. Monogamy of entanglement and teleportation capability . *Phys. Rev. Lett. 79* (2009), 042334.

[49] TURA, J., AUGUSIAK, R., SAINZ, A., VERTÉSI, T., LEWENSTEIN, M., AND ACÍN, A. Detecting non-locality in multipartite quantum systems with two-body correlation functions . *Science 344* (2014), 1256.

[50] VANDENBERGHE, L., AND BOYD, S. Semidefinite Programming . *SIAM Review 38*, 1 (1996), 49–95.

[51] WALDSPURGER, I., D'ASPREMONT, A., AND MALLAT, S. Phase recovery, maxcut and complex semidefinite programming. *Mathematical Programming* (2012), 1–35.

[52] WALLS, D. F., AND MILBURN, G. J. *Quantum Optics*, 2 ed. Springer Verlag, 2008.

[53] WATROUS, J. Semidefinite Programming - Lecture Notes., 2014. `https://cs.uwaterloo.ca/~watrous/CS766/LectureNotes/07.pdf`.

[54] WERNER, R. F., AND WOLF, M. M. Bell inequalities and entanglement. *Quantum. Inf. Comput. 1*, (3) (2002), 1.

[55] WOOTTERS, W. K., AND ZUREK, W. H. A single quantum cannot be cloned. *Nature 299* (1982), 802–803.

[56] WÜRFLINGER, L. E., BANCAL, J.-D., ACÍN, A., GISIN, N., AND VERTÉSI, T. Nonlocal multipartite correlations from local marginal probabilities . *Phys. Rev. A 86* (2012), 032117.

Acknowledgements

I would firstly like to thank my supervisor, Prof. Otfried Gühne for the support and patience shown during the time I have spent as a graduate student, as well as Prof. Thomas Mannel, for giving me a deeper insight into our particle physics problem.

I would also like to thank my colleagues, Felix Huber, Tristan Kraft, Jannik Hoffmann, Sabine Wölk, Costantino Budroni, Ali Asadian, Sanah Altenburg, Roope Uola, Mariami Gachechiladze, Nikolai Miklin, Christina Ritz, Nikolai Wyderka, Shin-Liang Chen, as well as former group members, Fabiano Lever, Frank Steinhoff, Tobias Moroder, Matthias Kleinmann, Martin Hofmann, for the truly wonderful time I have had while being a part of the Theoretical Quantum Optics group.

I thank Mrs. Daniela Lehmann for her support and help, especially when, more often than not, my administrative clumsiness made its presence felt.

Finally, I thank my wife, Diana, and my parents, for their love and support. Without them, this work would certainly not have been possible.

During my years as a doctoral student, I've met many people whom, in one way or another, have helped me in my endeavour. While apologizing for not being able to mention everyone in this small section, I sincerely thank them for all their efforts and good will.